

p-ISSN 2502-8952
e-ISSN 2623-2197

PENA TEKNIK



**JURNAL ILMIAH
ILMU-ILMU
TEKNIK**

**Diterbitkan:
Fakultas Teknik
Universitas Andi Djemma Palopo**

JIIT	Volume 10	Number 01	Page 1 - 56	March 2025	p-ISSN 2502-8952 e-ISSN 2623-2197
-------------	-----------	-----------	----------------	---------------	--------------------------------------

www.ojs.unanda.ac.id
email: penateknik@unanda.ac.id

EDITORIAL BOARD

Editor in Chief

Amiruddin Akbar Fisu

Universitas Andi Djemma, Indonesia

Managing Editor

Hisma Abduh

Universitas Andi Djemma, Indonesia

Board of Editors

Ahmad Ali Hakam Dani

Universitas Andi Djemma Palopo, Indonesia

Zulqadri Ansar

Technische Universität München, Germany

Rani Bastari Alkam

University of Nottingham, United Kingdom

Dwiana Novianti Tufail

Institut Teknologi Kalimantan, Indonesia

Gafar Lakatupa

Universitas Hasanuddin, Indonesia

Fitrawan Umar

Universitas Muhammadiyah Makassar, Indonesia

Dwinsani Pratiwi Astha

Universitas Tadulako, Indonesia

Feni Kurniati

Institut Teknologi Bandung, Indonesia

Apriyanto Apriyanto

Universitas Sulawesi Barat, Indonesia

Ahmad Fuad Zainuddin

Universitas Prasetiya Mulya, Indonesia

Asistant Editor

Amiul Amruh

Universitas Andi Djemma, Indonesia

Restu Restu

Universitas Andi Djemma, Indonesia

Reveiwers

Prof. Heru Purboyo Hidayat Putro	Institut Teknologi Bandung, Indonesia
Prof. Dr. Slamet Trisutomo	Universitas Hasanuddin, Indonesia
Erich Wolff	Nanyang Technological University, Singapore
Prince Winston D.	Kamaraj College of Engineering and Technology, India
Dasha Spasojevic	Monash University, Australia
Nga Nguyễn Thị Thu	Le Quy Don Technical University/LQDTU, Hanoi, Viet Nam
Olena V. Havrylenko	National Aerospace University "Kharkiv Aviation Institute", Ukraine
Qamar Ul Islam	Baba Ghulam Shah Badshah University, India
Ibnu Syabri	Institut Teknologi Bandung, Indonesia
Rossy Armyrn Machfudiyanto	Universitas Indonesia, Indonesia
Retantyo Wardoyo	Universitas Gadjah Mada, Indonesia
Windra Priatna Humang	Badan Riset dan Inovasi Nasional (BRIN), Indonesia
Ihsan Latief	Universitas Hasanuddin, Indonesia
I Gusti Ayu Andani	Institut Teknologi Bandung, Indonesia
Emil Salim Rasyidi	Universitas Bosowa, Makassar, Indonesia
Syafrianita Syafrianita	Universitas Logistik dan Bisnis Internasional, Indonesia
Arief Budiman	Universitas Sultan Ageng Tirtayasa, Indonesia
Jajan Rohjan	Universitas Pasundan, Indonesia
Ringgy Masuin	Ministry of Public Works and Public Housing, Indonesia
Dwi Novirani	Institut Teknologi Nasional, Bandung, Indonesia
Kelik Sussolaikah	Universitas PGRI Madiun
Nahdalina Nahdalina	Universitas Gunadarma, Indonesia
Nurul Wahjuningsih	Institut Teknologi Bandung, Indonesia
Imam Sonny	Research and Development Agency, Ministry of Transportation, Indonesia
Johny Malisan	Research and Development Agency, Ministry of Transportation, Indonesia
Dadang Iskandar	Universitas Muhammadiyah Metro, Indonesia

TABLE OF CONTENTS

Ariawan Bayu Wicaksono, Muh. Abdillah Muh. Abdillah, Ishak Ishak, Nurhidayanti Nurhidayanti

1-13

Density Influence on Acoustic Performance of Waste Composite Materials

DOI: https://doi.org/10.51557/pt_jiit.v10i1.3037

Bulgis Bulgis, Salim Salim, Yogi Nauvally, Muh. Riyan

14-24

Deformation Resistance of Stone Mastic Asphalt Mixtures With Fiber Mesh Added Materials

DOI: https://doi.org/10.51557/pt_jiit.v10i1.2539

Jansen Briano, Kornelius Sophiano Tanuwidjaja, Yosia Gabriel Kurniawan, Meyland Meyland, Samuel Pangeran Aletheia

25-38

Pre-Design and Environmental Impact Analysis of Methanol Plant from Natural Gas with Dielectric Barrier Discharge Reactor

DOI: https://doi.org/10.51557/pt_jiit.v10i1.2950

Nurhidayanti Nurhidayanti, Muhammad Ikhsan, Budiawan Sulaeman

39-45

Experimental Laser Cutting Material Removal Rate for Polymethylmethacrylate in Construction Applications

DOI: https://doi.org/10.51557/pt_jiit.v10i1.3074

Azizah Putri Abdi, Rasdiana Rasdiana, Yan Radhinal, Tri Wahyuningsih, Andi Idham Asman

46-56

Sustainability Strategy for Makassar City Central Waste Bank

DOI: https://doi.org/10.51557/pt_jiit.v10i1.3156

Density Influence on Acoustic Performance of Waste Composite Materials

Ariawan Bayu Wicaksono^{1,*}, Muh. Abdillah¹, Ishak¹, Nurhidayanti¹,

¹ Mechanical Engineering, Politeknik Negeri Ujung Pandang, Makassar, Indonesia

* Corresponding Author E-mail: ariawanbayu@poliupg.ac.id

Abstract

This study aimed to determine the effect of material density on the sound absorption coefficient (SAC) of composite materials made from rice husk, rice straw, and sawdust. Rice husk, rice straw, and sawdust were made into composite materials with volume fraction variations of 30:70, 25:75, and 20:80 with a thickness of 25 mm. The samples were tested in the 200–1600 Hz frequency range using two microphones and a type 4206 impedance tube in accordance with ASTM E1050 standards. The test findings showed that the composite material made of rice straw had the best SAC at 1600 Hz with an α value of 0.72 and a volume fraction variation of 30:70, probably because it was less dense than the other materials. The maximum SAC values for the 30:70 volume fraction variation were 0.72 for the rice straw composite material at 1600 Hz, 0.42 for the rice husk composite material at the same frequency, and 0.13 for the sawdust material at 1000 Hz. The discussion leads one to believe that the SAC is heavily influenced by the bulk density of the forming fiber material and the density that is generated by the fluctuation in volume fraction of a composite material

Keywords:

Composite materials; sound absorption; rice husk; rice straw; sawdust

1. INTRODUCTION

Agricultural waste in Indonesia, especially rice straw, rice husks, and sawdust, has become a significant environmental issue. In the last five years, Indonesia's total rice production reached around 56 million tons, generating rice straw waste equivalent to about 22 million tons annually. Rice husks are also a concern, with production reaching more than 16 million tons based on BPS 2022 data (Nadiyya et al., 2022). These wastes are often burned, producing emissions that potentially pollute the air and pose a risk to public health. Research shows that the burning of agricultural waste contributes approximately 15% of the total air pollution in Indonesia, which can lead to health problems, including respiratory disorders and chronic diseases in the exposed population (Ariyanto et al., 2022).

However, Indonesia's noise pollution problem is also growing in importance. Surveys conducted over the last five years have revealed that over 80% of urban dwellers are subjected to noise levels above the permissible threshold of 70 dB. Public health is negatively impacted by this noise pollution, which leads to stress, sleep disorders, and other mental health problems (Zullaikah et al., 2022). With peak noise levels of 85 dB, Jakarta is among the cities with the highest noise levels, according to data from the Ministry of Environment and Forestry (Nabila et al., 2024). Additionally, excessive noise has an adverse effect on public health and quality of life, which can result in financial losses because of higher medical expenses (Zullaikah et al., 2022).

The importance of managing agricultural waste and noise pollution simultaneously drives innovation to utilize agricultural waste as sound-absorbing material. Research shows that agricultural waste-based materials, such as composites made from rice straw, rice husks, and wood dust, can function as effective sound insulators. The density of the material directly contributes to its acoustic performance; the higher the density, the better the acoustic performance, as demonstrated in the research by Zullaikah et al. who found a positive correlation between composite density and sound absorption capability (Zullaikah et al., 2021; Suliartini et al., 2023; Wicaksono et al., 2023).

Thus, this research needs to be more in-depth to explore the potential of agricultural waste in reducing dependence on conventional raw materials while providing solutions to existing noise pollution problems. This effort is expected to create synergy between the environment and waste utilization for the advancement of the eco-friendly industry in Indonesia.

2. METHODS

The process of composite fabrication is conducted using a mold, followed by application of pressure for a specified duration. Subsequently, an impedance tube with two microphones is used to conduct sound absorption testing in the 200 - 1600 Hz range in accordance with the ASTM E1050 standard.

2.1 Reinforcing Material

Composites are composed of two primary components, a matrix and a reinforcing substance. A variety of fibers can be used as the reinforcing material, which may be either synthetic or natural. In this research, natural fibers were utilized, specifically rice straw, rice husks, and sawdust, as illustrated in Figures 1, 2, and 3. In most cases, resins and catalysts make up the matrix, which binds the fibers together.



Figure 1. Rice straw material



Figure 2. Rice husks material



Figure 3. Sawdust material

Many applications rely on the densities of rice husk, sawdust, and straw, especially in the building and materials science domains. Rice husk has a bulk density that typically ranges from 85 to 110 kg/m³, depending on its moisture content and processing methods (Milawarni, 2023; Missagia et al., 2011). In contrast, sawdust generally exhibits a higher density, which can vary significantly based on the type of wood and processing techniques, with reported values ranging from 160 to 800 kg/m³ (Rumaizah et al., 2019; Stasiak et al., 2015). Rice straw, on the other hand, has a bulk density that falls between these two materials, typically around 162 to 194 kg/m³ (Zhang et al., 2012). The rice straw's density can also be influenced by its particle size and moisture content, which are critical factors in its application as a biomass energy source or in composite materials (Zhang et al., 2012). Understanding these density variations is crucial for optimizing the use of these agricultural by-products in sustainable construction and energy applications.

Farmers in Sidrap, South Sulawesi, Indonesia, provided the rice straw used in this research. The straw had a bulk density of 110 kg/m³ and was about 50 to 70 cm long. Similarly, the rice husks were also procured from farmers in Sidrap, South Sulawesi, with a bulk density of 138 kg/m³ and dimensions of about 10 mm in length and 3 mm in width. The sawdust utilized in this study was derived from waste generated during furniture manufacturing, exhibiting a bulk density of 214 kg/m³.

2.2 Matrix

The research employs Yukalac 157 BQTN-EX polyester resin, which is useful in a number of ways: it is inexpensive, easy to get, has low viscosity, high mechanical strength, and great environmental resistance. This resin is particularly noted for its application in composite materials due to its favorable characteristics, which enhance processing and performance in various applications (Murdani et al., 2017; Sasria, 2022). Furthermore, the catalyst employed in this study is Methyl Ethyl Ketone Peroxide (MEKP), which is commonly used to initiate the curing process in polyester resins (Herwandi & Napitupulu, 2017; Sasria, 2022). Figure 4 shows the resin used in the study, whereas Figure 5 shows the catalyst.



Figure 4. Yukalac 157 BQTN-EX resin



Figure 5. Methyl Ethyl Ketone Peroxide catalyst

2.3 Fibre Treatment

Composite panels begin with materials that have undergone an initial treatment procedure; these materials include rice husk, sawdust, and straw. Initially, these materials undergo a washing procedure with distilled water to eliminate any dust and dirt contaminants. Following this, the rice straw and rice husks are subjected to solar drying for a duration of 48 hours to facilitate moisture removal. After that, after two hours in an electric oven set at 100°C, dry the rice straw and husks. Doing so will aid in further decreasing the materials' moisture content. To make sure the rice straw will fit in the oven, it is first chopped into sections that are about 20 to 25 centimeters in length. After the oven drying phase, the rice straw is then cut into smaller pieces ranging from 3 to 5 cm to promote uniform distribution during the molding of the composite panels.

2.4 Mould for Composite Panels

The dimensions of the mold used for molding composite panels are 300 mm x 300 mm x 45 mm, and an inner limiting iron or stopper with dimensions of 280 mm x 20 mm x 25 mm is also required. Figure 6 shows the design of the composite panel mold that was used in this inquiry, while Figure 7 shows the design of the composite panel mold that was not.



Figure 6. Design of a composite panel mould



Figure 7. Mould for composite panels

2.5 Composite Panel Manufacturing

The following phase, following the preparation of the composite panel molds, is to gather the ingredients and tools needed for mixing. Three different volume fractions were employed in this investigation. The first volume fraction, which consists of fibers, was set at 30%, while the matrix constituted 70% of the total composition. The second volume fraction, also comprising fibers, was established at 25%, with the matrix making up 75% of the total composition. The third volume fraction, which consists of 20% fiber and 80% matrix. To ensure accurate measurements, a scale and graduated cylinder were employed to measure the amounts of fibers and matrix separately. Initially, the fibers and matrix must be placed in separate containers.

The catalyst used in this study was measured at 2% of the total volume of the matrix. This catalyst was subsequently added to the resin solution, followed by thorough stirring to achieve a uniform mixture between the resin and catalyst for five minutes. Afterward, the matrix was poured into the container containing the fibers, and both components were mixed by hand until they were evenly combined. Because the resin can irritate the skin and cause burning and itching, it is essential to wear gloves throughout the process.

Once the mixture of fibers and matrix is adequately blended, it is introduced into the composite panel mold, ensuring that the mixture is evenly distributed and leveled, as illustrated in Figures 8, 9, and 10. Before placing the fiber and matrix mixture into the composite panel mold, it is essential to apply a Release Agent to all mold surfaces to facilitate the removal of the composite panel after curing. After applying the release agent, the mold is closed and placed under a press. Figure 11 shows the next step, which is to put the composite panel mold under pressure for 24 hours using a 3,000 psi jack pressure load.



Figure 8. Rice straw and matrix mixture



Figure 9. Rice husks and matrix mixture



Figure 10. sawdust and matrix mixture



Figure 11. Pressing procedure for moulding composite panels

Upon the conclusion of the composite panel molding procedure, the next step involves disassembling the mold and extracting the completed composite panel from it. Subsequently, allow the composite panels to thoroughly dry for a duration of 1 to 2 hours at ambient temperature.

2.6 Preparing The Sample

Following the molding of the composite panels, the subsequent phase involves the preparation of samples. Initially, as seen in Figures 12, 13, and 14, the composite material is cut into 100 mm diameter circles.



Figure 12. Rice straw composite material sample (RS)



Figure 13. Rice husk composite material sample (RH)



Figure 14. Sawdust composite material sample (SD)

2.7 Test for Sound Absorption

According to the ASTM E1050, a two-microphone impedance tube was utilized in this work to assess the absorption and impedance characteristics of the acoustic materials (ASTM E 1050, 1998). This impedance tube technique is favored in research settings due to its efficiency, as it necessitates a brief testing duration and requires only a small sample size. In this study, the Brüel & Kjaer impedance tube kit was used. It includes a 4206-type impedance tube, two 4187-type 1/4 inch condenser microphones, a 2716C amplifier, and a 3160-A-042 Xi LAN acquisition module. Through the use of PULSE LabShop software version 1.16.0, this configuration is connected to a personal computer. The basic idea behind this technique is to put the sample material at one end of an impedance tube and the sound source (loudspeaker) at the other. As they pass through the tube, the loudspeaker's haphazardly generated sound waves, interact with the sample, and subsequently reflect back, as depicted in the schematic diagram in Figure 16 (Çelikel & Babaarslan, 2017).

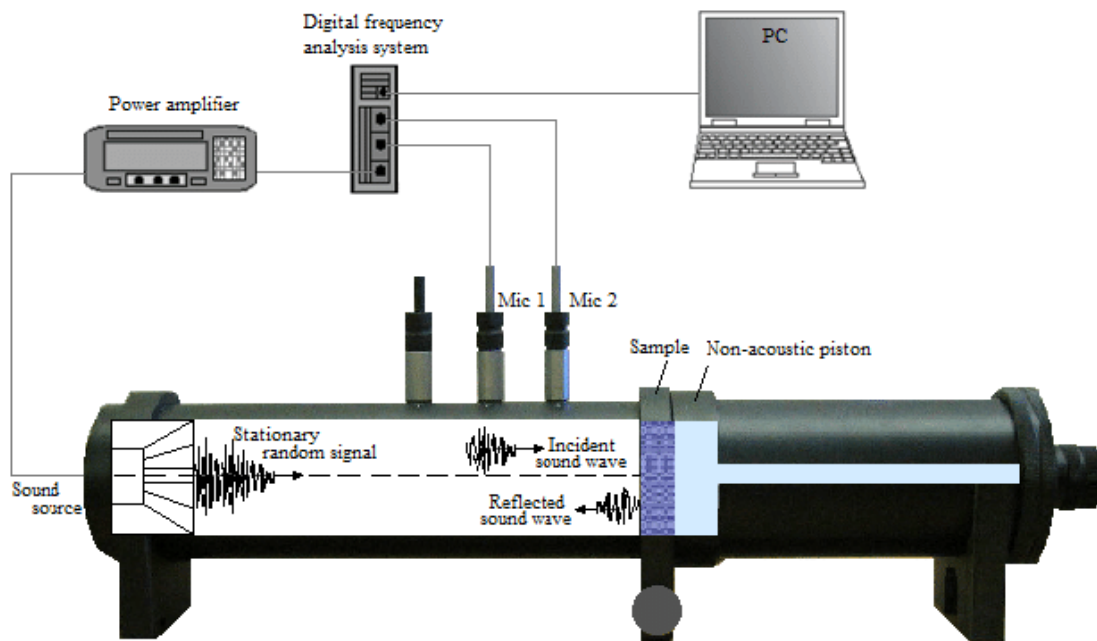


Figure 16. Brüel & Kjaer impedance tube kit schematic diagram (Çelikel & Babaarslan, 2017)

The sample used in the testing procedure has a diameter of 100 mm. The specimen is placed at one end of a tube and then linked to another tube. The adjustment process and microphone calibration follow the joining of the two tubes. Following these pre-test procedures, the sample is subjected to the sound absorption test. Sound absorption measurements will be recorded at frequencies between 200 and 1,600 Hz as part of this study. Figures 18, 19, and 20 show the sample's placement within the impedance tube, while Figure 17 shows the impedance tube used in this study.



Figure 17. The Impedance tube kit from Brüel & Kjaer



Figure 18. Mounted composite sample of rice straw



Figure 19. Mounted composite sample of rice husk

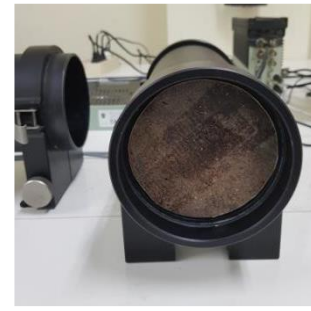


Figure 20. Mounted composite sample of sawdust

3. RESULT AND DISCUSSION

The authors of this study plotted the density against the SAC to show how the two variables relate to one another. The specific gravity of the fiber materials utilized, which include rice husk (RH), sawdust (SD), and rice straw (RS), indirectly affects density. Figure 21 and Table 1 show the noise absorption coefficients produced by the composite materials of sawdust, rice straw, and rice husk with a volume fraction of 30:70 and a thickness of 25 mm (T25), for example.

Table 1. SAC of composite materials with 30:70 fraction volume

Frequency (Hz)	SAC (α)			Frequency (Hz)	SAC (α)		
	30 : 70				30 : 70		
	RS	RH	SD		RS	RH	SD
200	0.12	0.06	0.01	1000	0.37	0.18	0.13
300	0.22	0.13	0.01	1100	0.36	0.17	0.12
400	0.36	0.25	0.01	1200	0.37	0.17	0.10
500	0.48	0.39	0.02	1300	0.36	0.19	0.07
600	0.47	0.40	0.02	1400	0.42	0.21	0.06
700	0.43	0.32	0.03	1500	0.51	0.28	0.07
800	0.41	0.24	0.05	1600	0.72	0.42	0.11
900	0.39	0.20	0.09				

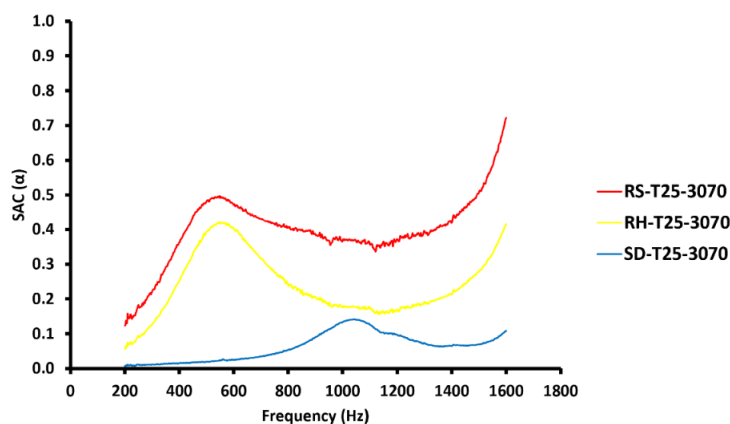


Figure 21. SAC of composite materials with 30:70 fraction volume

Based on Table 1 and Figure 21, it can be observed that rice straw composite materials exhibit the highest noise absorption coefficient across all frequencies, achieving a maximum value of α at 1600 Hz of 0.72. This is followed by rice husk composite materials, which have the second highest noise absorption coefficient, reaching a peak value of α at 1600 Hz of 0.42. Lastly, sawdust composite materials demonstrate the lowest noise absorption coefficient, with max α value at 1000 Hz of 0.13. Figure 22 and Table 2 show the noise

absorption coefficients produced by rice husk (RH), sawdust (SD), and rice straw composite (RS) materials with a volume fraction of 25:75 and 25 mm (T25), respectively.

Table 2. SAC of composite materials with 25:75 fraction volume

Frequency (Hz)	SAC (α)			Frequency (Hz)	SAC (α)		
	25 : 75				25 : 75		
	RS	RH	SD		RS	RH	SD
200	0.04	0.02	0.01	1000	0.23	0.15	0.06
300	0.07	0.04	0.01	1100	0.23	0.14	0.09
400	0.12	0.07	0.02	1200	0.23	0.14	0.10
500	0.20	0.11	0.02	1300	0.25	0.15	0.12
600	0.28	0.17	0.02	1400	0.27	0.15	0.11
700	0.30	0.24	0.03	1500	0.32	0.16	0.10
800	0.28	0.19	0.04	1600	0.41	0.20	0.11
900	0.26	0.15	0.05				

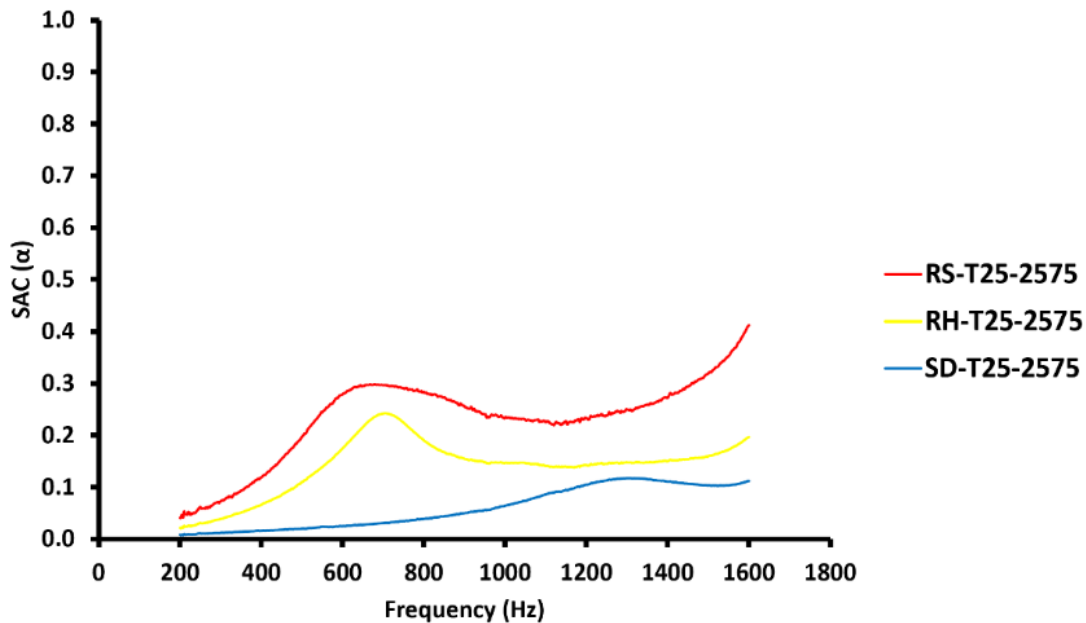


Figure 22. SAC of composite materials with 25:75 fraction volume

Based on the findings presented in Table 2 and Figure 22, The best noise absorption coefficient across all frequencies is clearly demonstrated by rice straw composite materials, achieving a maximum value of α at 1600 Hz of 0.41. This is followed by rice husk composite materials, which have the second highest noise absorption coefficient, reaching a peak value of α at 700 Hz of 0.24. Lastly, sawdust composite materials demonstrate the lowest noise absorption coefficient, with a maximum α value at 1300 Hz of 0.12.

Based on the data presented in Table 1, Figure 21, Table 2, and Figure 21, we can conclude that each constituent material used in the composite significantly influences metrics for the composite material's sound absorption coefficient (SAC). We are aware that the bulk density of the sawdust and rice husk materials is higher than that of the rice straw material, which is lower at 110 kg/m³. The next densest material is sawdust, with a bulk density of 214 kg/m³, followed by rice husk material with a density of 138 kg/m³. Ultimately, it may be said that a composite material's SAC is directly proportional to its bulk density, and that the reverse is also true.

Composites' overall mass density significantly influences their sound absorption coefficients, with optimal density levels being crucial for maximizing acoustic performance. Higher bulk densities often correlate with reduced porosity, leading to diminished sound absorption capabilities due to the smaller pore sizes that are

essential for effective sound wave dissipation (Chanlert et al., 2022; Lyu et al., 2019). For instance, studies have shown that composites with increased flow resistivity and tortuosity, resulting from higher bulk density, hinder sound wave propagation, causing more energy loss through friction (Jang, 2023; Prabowo et al., 2019). Conversely, materials with lower bulk density tend to exhibit higher porosity, which enhances their sound-absorbing abilities (Chanlert et al., 2022). Additionally, the relationship between density and sound absorption is complex “while higher density can improve performance at certain frequencies, it may also lead to suboptimal absorption at others, particularly in low-frequency ranges” (Lyu et al., 2021; Sakagami et al., 2019). Therefore, careful consideration of bulk density is essential in the design of composite materials aimed at optimizing sound absorption properties.

Figure 23 and Table 3 show the corresponding results for the sound absorption coefficient values produced by rice straw composite material with a 25 mm thickness and volume fraction variations of 30:70, 25:75, and 20:80, respectively.

Table 3. SAC of rice straw composite material with 30:70, 25:75, and 20:80 fraction volume

Frequency (Hz)	SAC (α)			Frequency (Hz)	SAC (α)		
	RS				RS		
	30 : 70	25 : 75	20 : 80		30 : 70	25 : 75	20 : 80
200	0.12	0.04	0.01	1000	0.37	0.23	0.08
300	0.22	0.07	0.01	1100	0.36	0.23	0.11
400	0.36	0.12	0.01	1200	0.37	0.23	0.12
500	0.48	0.20	0.02	1300	0.36	0.25	0.10
600	0.47	0.28	0.02	1400	0.42	0.27	0.09
700	0.43	0.30	0.03	1500	0.51	0.32	0.10
800	0.41	0.28	0.04	1600	0.72	0.41	0.14
900	0.39	0.26	0.05				

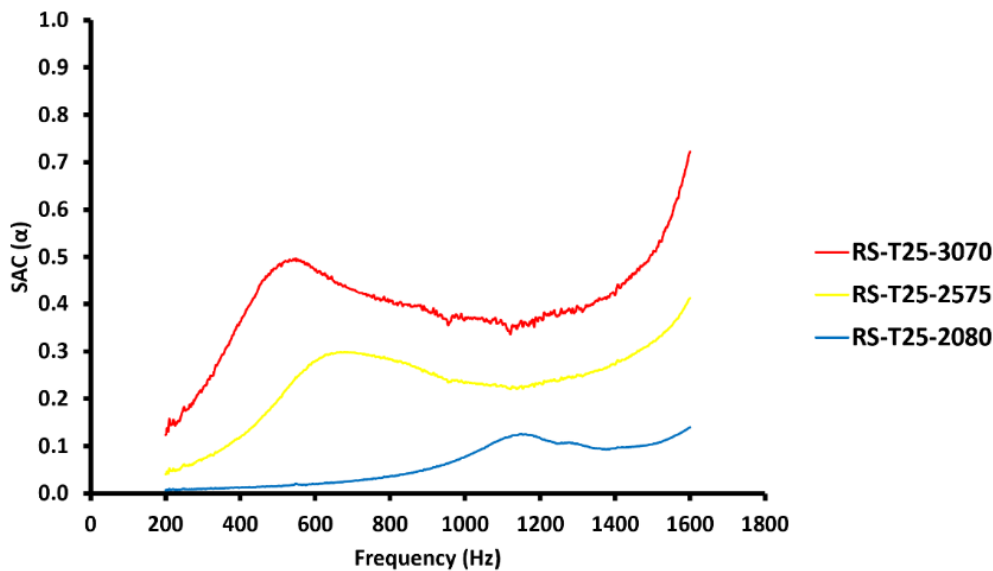


Figure 23. SAC of rice straw composite material with 30:70, 25:75, and 20:80 fraction volume

From the data shown in Table 3 and Figure 23, we can see that the rice straw composite material with a volume fraction variation of 30:70 has the highest SAC at every frequency compared to the volume fraction variations of 25:75 and 20:80, with the highest noise absorption coefficient at a frequency of 1600 Hz with an α value of 0.72. This is followed by the volume fraction variation of 25:75, which has the second-highest noise absorption coefficient, with the highest noise absorption coefficient at a frequency of 1600 Hz with an α value of 0.41. Lastly, the volume fraction of 20:80 has the lowest noise absorption coefficient, with the highest noise absorption coefficient at a frequency of 1600 Hz with an α value of 0.14. The comparison data of the noise

absorption coefficients produced by the rice husk composite material (RH) with a thickness of 25 mm, and with volume fraction variations of 30:70, 25:75, and 20:80 are shown in Table 4 and Figure 24, respectively.

Table 4. SAC of rice husk composite material with 30:70, 25:75, and 20:80 fraction volume

Frequency (Hz)	SAC (α)			Frequency (Hz)	SAC (α)		
	RH				RH		
	30 : 70	25 : 75	20 : 80		30 : 70	25 : 75	20 : 80
200	0.06	0.02	0.01	1000	0.18	0.15	0.15
300	0.13	0.04	0.02	1100	0.17	0.14	0.14
400	0.25	0.07	0.02	1200	0.17	0.14	0.12
500	0.39	0.11	0.03	1300	0.19	0.15	0.10
600	0.40	0.17	0.05	1400	0.21	0.15	0.09
700	0.32	0.24	0.07	1500	0.28	0.16	0.09
800	0.24	0.19	0.10	1600	0.42	0.20	0.13
900	0.20	0.15	0.13				

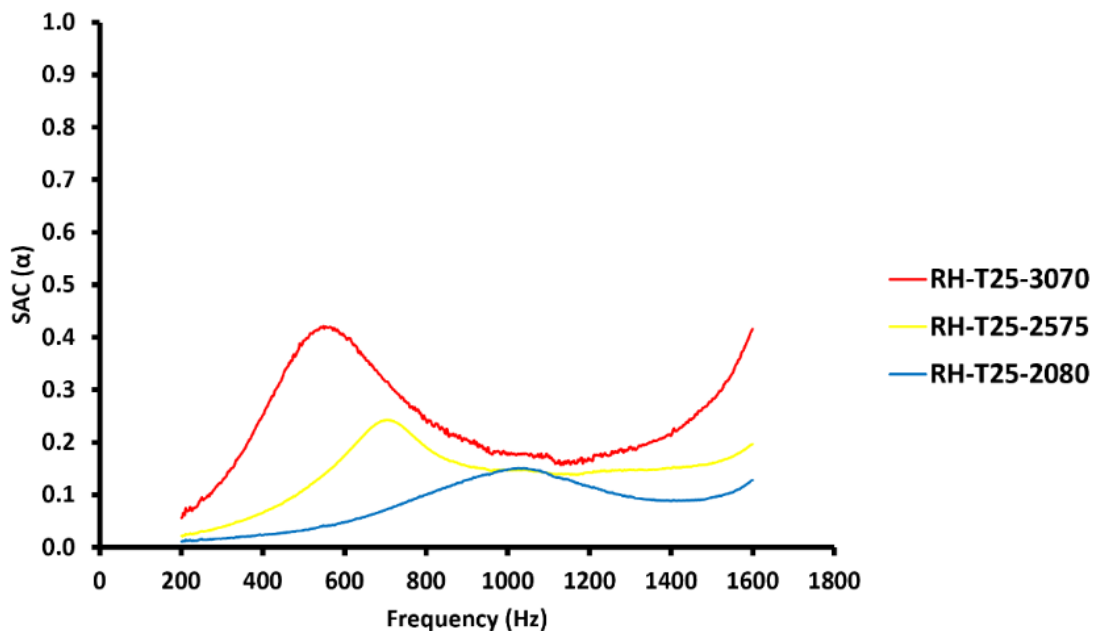


Figure 24. SAC of rice husk composite material with 30:70, 25:75, and 20:80 fraction volume

From the data shown in Table 4 and Figure 24, at all frequencies, the 30:70 volume fraction variation of the rice husk composite material has the highest noise absorption coefficient (NAC), in comparison to the 25:75 and 20:80 volume fraction variations. The highest noise absorption coefficient, with an α value of 0.42, was observed at 1600 Hz. Right after that comes the 25:75 volume fraction fluctuation, which has the second-highest noise absorption coefficient. The maximum noise absorption coefficient, with an α value of 0.24, occurs at a frequency of 700 Hz. Finally, at a frequency of 1000 Hz, with an α value of 0.15, the noise absorption coefficient is maximum for the volume fraction of 20:80, which also has the lowest value overall. After that, Table 5 and Figure 25 exhibit the comparison data of the noise absorption coefficients produced by the sawdust composite material (SD) with a thickness of 25 mm and with volume fraction changes of 30:70, 25:75, and 20:80, respectively.

Table 5. SAC of sawdust composite material with 30:70, 25:75, and 20:80 fraction volume

Frequency (Hz)	SAC (α)			Frequency (Hz)	SAC (α)		
	SD				SD		
	30 : 70	25 : 75	20 : 80		30 : 70	25 : 75	20 : 80
200	0.01	0.01	0.00	1000	0.13	0.06	0.03
300	0.01	0.01	0.01	1100	0.12	0.09	0.04
400	0.01	0.02	0.01	1200	0.10	0.10	0.04
500	0.02	0.02	0.01	1300	0.07	0.12	0.04
600	0.02	0.02	0.01	1400	0.06	0.11	0.05
700	0.03	0.03	0.01	1500	0.07	0.10	0.07
800	0.05	0.04	0.02	1600	0.11	0.11	0.09
900	0.09	0.05	0.03				

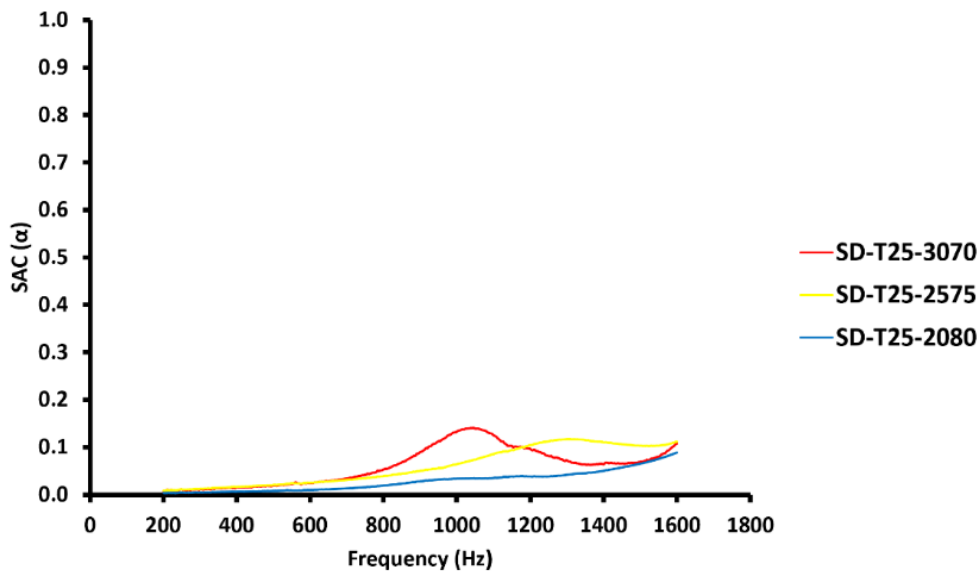


Figure 25. SAC of sawdust composite material with 30:70, 25:75, and 20:80 fraction volume

From the data shown in Table 5 and Figure 25, in the mid-frequency region, particularly at a frequency of 1000 Hz with a value of α equal to 0.13, the composite material of sawdust exhibits the highest sound absorption coefficient (SAC), as can be seen from the volume fraction fluctuation of 30:70. The noise absorption coefficient is highest at a frequency of 1300 Hz, with a value of α equal to 0.12, for the high-frequency range, in the material with a volume percent variation of 25:75, and when reaching the highest frequency of 1600 Hz, the composite materials with volume fraction variations of 30:70 and 25:75 have the same α value of 0.11. Finally, the composite material with a volume fraction variation of 20:80 is the material with the lowest noise absorption value, with the highest noise absorption value at a frequency of 1600 Hz with a value of α equal to 0.09.

From the data of composite materials with variations in the volume fraction between the fibers and the matrix, it can be concluded that the greater the matrix ratio, the higher the SAC produced by the composite material. The SAC of composite materials, particularly those incorporating fibers and polyester resin, is significantly influenced by the volume fraction of fibers and the type of resin used.

Research indicates that increasing the fiber volume fraction generally enhances the SAC due to increased porosity and surface area, with optimal results often found at specific ratios, such as 30% for banana fibers (Fauziah et al., 2022). Additionally, the inherent properties of the fibers, such as density and length, play a critical role in acoustic performance, with different fibers yielding varying SAC values (Indrawati, 2023). For instance, coir fibers exhibit distinct acoustic absorption characteristics compared to other natural fibers, although specific comparisons with date palm fibers require further investigation (Taban et al., 2021).

Furthermore, the interaction between fiber characteristics and resin content is crucial “higher fiber content can lead to improved sound absorption, particularly at lower frequencies” (Süvari & Dulek, 2019). Overall, the relationship between fiber volume fraction and SAC is complex, necessitating careful optimization to achieve desired acoustic properties in composite materials (Hassan et al., 2021; Lyu et al., 2019).

4. CONCLUSIONS

At a frequency of 1600 Hz, the composite material made of rice straw yields the maximum SAC value ($\alpha = 0.72$) with a volume fraction variation of 30:70. This is because rice straw material has a lower bulk density compared to rice husk and sawdust materials. The smaller the bulk density value of a material, the higher the porosity of the material, which will improve the sound absorption coefficient value. The 30:70 volume fraction variation is an excellent ratio and has the highest SAC value, namely an α value of 0.72 for the rice straw composite material at a frequency of 1600 Hz, 0.42 for the rice husk composite material at a frequency of 1600 Hz, and 0.13 for the sawdust composite material at a frequency of 1000 Hz. The volume fraction variation also significantly affects the sound absorption coefficient value indirectly. The more resin used, the higher the density of a composite material, as a consequence, the composite material's porosity will decrease and the sound absorption coefficient will be lower. Therefore, it can be concluded that the bulk density of the forming fiber material and the density formed by the variation in volume fraction of a composite material significantly affect the resulting sound absorption coefficient.

5. ACKNOWLEDGMENTS

I wish to extend my sincere gratitude to all my esteemed colleagues who have participated and provided invaluable assistance throughout the research process.

REFERENCES

- Ariyanto, S. R., Dianastiti, Y., Cahyadi, W., Nugraha, A. S., & Pratama, M. (2022). Pelatihan Pembuatan Biobriket Arang Sekam Padi Untuk Meningkatkan Ekonomi Masyarakat Desa Doroampel Kabupaten Tulungagung. *Jurnal Pengabdian Masyarakat Sains Dan Teknologi*, 1(4), 112–121. <https://doi.org/10.58169/jpmsaintek.v1i4.67>
- ASTM E 1050. (1998). Standard test method for impedance and absorption of acoustical materials using a tube, two microphones and a digital frequency analysis system. *American Society for Testing of Materials, C*, 1–12.
- Çelikel, D. C., & Babaarslan, O. (2017). Effect of bicomponent fibers on sound absorption properties of multilayer nonwovens. *Journal of Engineered Fibers and Fabrics*, 12(4), 15–25. <https://doi.org/10.1177/155892501701200403>
- Chanlert, P., Jintara, A., & Manoma, W. (2022). Comparison of the Sound Absorption Properties of Acoustic Absorbers Made From Used Copy Paper and Corrugated Board. *Bioresources*, 17(4), 5612–5621. <https://doi.org/10.15376/biores.17.4.5612-5621>
- Fauziah, R., Ramli, R., Darvina, Y., & Ratnawulan, -. (2022). Effect of the Volume of Banana Fiber as a Polymer Composite Amplifier With Polyester Resin Matrix on the Sound Absorption of Acoustic Materials. *Pillar of Physics*, 15(1). <https://doi.org/10.24036/12561171074>
- Hassan, T., Jamshaid, H., Mishra, R., Khan, M. Q., Petru, M., Tichý, M., & Müller, M. (2021). Factors Affecting Acoustic Properties of Natural-Fiber-Based Materials and Composites: A Review. *Textiles*, 1(1), 55–85. <https://doi.org/10.3390/textiles1010005>
- Herwandi, H., & Napitupulu, R. (2017). Pengaruh Peningkatan Kualitas Serat Resam Terhadap Kekuatan Tarik, Flexure Dan Impact Pada Matriks Polyester Sebagai Bahan Pembuatan Dashboard Mobil. *Turbo Jurnal Program Studi Teknik Mesin*, 4(2). <https://doi.org/10.24127/trb.v4i2.72>

- Indrawati, S. (2023). Effect of Fiber's Size on Acoustic Absorption of Abaca Fiber/Epoxy Resin Composites. *Key Engineering Materials*, 951, 59–64. <https://doi.org/10.4028/p-n7buxr>
- Jang, E. S. (2023). Sound Absorbing Properties of Selected Green Material—A Review. *Forests*, 14(7), 1366. <https://doi.org/10.3390/f14071366>
- Lyu, L., Liu, Y., Bi, J., & Guo, J. (2019a). Sound Absorption Properties of DFs/EVA Composites. *Polymers*, 11(5), 811. <https://doi.org/10.3390/polym11050811>
- Lyu, L., Zhang, D., Tian, Y., & Zhou, X. (2021). Sound-Absorption Performance and Fractal Dimension Feature of Kapok Fibre/Polycaprolactone Composites. *Coatings*, 11(8), 1000. <https://doi.org/10.3390/coatings11081000>
- Milawarni, M. (2023). Analysis of Physical and Mechanical Properties of Rice Husk-Based Particle Board. *Journal of Advanced Research in Applied Sciences and Engineering Technology*, 31(3), 43–49. <https://doi.org/10.37934/araset.31.3.4349>
- Missagia, B., Guerrero, C., Narra, S., Sun, Y., Ay, P., & Krautz, H. J. (2011). Physicomechanical Properties of Rice Husk Pellets for Energy Generation. *Energy & Fuels*, 25(12), 5786–5790. <https://doi.org/10.1021/ef201271b>
- Murdani, A., Hadi, S., & Amrullah, U. S. (2017). Flexural Properties and Vibration Behavior of Jute/Glass/Carbon Fiber Reinforced Unsaturated Polyester Hybrid Composites for Wind Turbine Blade. *Key Engineering Materials*, 748, 62–68. <https://doi.org/10.4028/www.scientific.net/kem.748.62>
- Nabila, S. A., Rahmiwati, A., Novrikasari, N., & Sunarsih, E. (2024). Perilaku Pola Makan Dan Aktivitas Fisik Terhadap Masalah Obesitas : Systematic Review. *Media Publikasi Promosi Kesehatan Indonesia (Mppki)*, 7(3), 498–505. <https://doi.org/10.56338/mppki.v7i3.4533>
- Nadiyya, A., Laila, L. L., Nashiroh, P. K., Mawanta, E., & Wahyu, A. T. (2022). Pemberdayaan Karang Taruna Melalui Pelatihan Pemanfaatan Limbah Sekam Padi Menjadi Briket Bioarang Di Desa Gumul, Kabupaten Klaten. *Budimas Jurnal Pengabdian Masyarakat*, 4(2). <https://doi.org/10.29040/budimas.v4i2.6649>
- Prabowo, A. E., Diharjo, K., Ubaidillah, U., & Prasetyo, I. (2019). Sound Absorption Performance of Sugar Palm Trunk Fibers. *E3s Web of Conferences*, 130, 01003. <https://doi.org/10.1051/e3sconf/201913001003>
- Rumaizah, C. Z., Azaman, F., Hasmizam, R. M., Asmadi, A., & Nor, M. A. A. M. (2019). Properties and Filtration Performance of Porous Clay Membrane Produced Using Sawdust as Pore Forming Agent. *Key Engineering Materials*, 821, 337–342. <https://doi.org/10.4028/www.scientific.net/kem.821.337>
- Sakagami, K., Okuzono, T., Somatomo, Y., Funahashi, K., & Toyoda, M. (2019). A Basic Study on a Rectangular Plane Space Sound Absorber Using Permeable Membranes. *Sustainability*, 11(7), 2185. <https://doi.org/10.3390/su11072185>
- Sasria, N. (2022). Composite Manufacturing of Coir Fiber-Reinforced Polyester as a Motorcycle Helmet Material. *JMPM (Jurnal Material Dan Proses Manufaktur)*, 6(1). <https://doi.org/10.18196/jmpm.v6i1.13756>
- Stasiak, M., Molenda, M., Bańda, M., & Gondek, E. (2015). Mechanical Properties of Sawdust and Woodchips. *Fuel*, 159, 900–908. <https://doi.org/10.1016/j.fuel.2015.07.044>
- Suliantini, N. W. S., Irmayani, I., Maisopa, I., Ismayanti, J., Khairina, K., AP, J. A., Ramadhan, D. A., Ali, K. O., Sintanu, Muh. A. W., Alvin, Z., & Mukmin, A. (2023). Sosialisasi Pengelolaan Limbah Peternakan Dan Pertanian Untuk Meningkatkan Kesehatan Masyarakat Di Desa Batu Kumbang Kecamatan Lingsar. *Jurnal Abdi Insani*, 10(4), 2811–2819. <https://doi.org/10.29303/abdiinsani.v10i4.1282>
- Süvari, F., & Dulek, Y. (2019). Investigating the Effect of Raising on the Sound Absorption Behavior of Polyester Woven Fabrics. *Textile Research Journal*, 89(23–24), 5119–5129. <https://doi.org/10.1177/0040517519848161>
- Taban, E., Amininasab, S., Mehrzad, S., Fattahi, M., Tajik, L., & Samaei, S. E. (2021). Comparison of Experimental and Empirical Approaches for Determination of Sound Absorption Properties of Bagasse and Cornhusk Fibers. *Journal of Natural Fibers*, 19(14), 9024–9038. <https://doi.org/10.1080/15440478.2021.1982108>

- Wicaksono, A., Djafar, Z., & Kusno, A. (2023). Sound Absorption Coefficient Analysis for Composite Made of Agricultural Waste. *Materials Science Forum*, 1091, 161–170. <https://doi.org/10.4028/p-mo2395>
- Zhang, Y., Ghaly, A. E., & Li, B. (2012). Physical Properties of Rice Residues as Affected by Variety and Climatic and Cultivation Conditions in Three Continents. *American Journal of Applied Sciences*, 9(11), 1757–1768. <https://doi.org/10.3844/ajassp.2012.1757.1768>
- Zullaikah, S., Jannah, A., Pramujati, B., P., E. N., & Haryanto, H. (2021). Teknologi Pembuatan Pakan Ternak Ruminansia Murah Dan Mudah Berbasis Limbah Pertanian Yang Ramah Lingkungan. *Sewagati*, 5(2), 112. <https://doi.org/10.12962/j26139960.v5i2.8097>
- Zullaikah, S., Pramujati, B., Prasetyo, E. N., Jannah, A., Wicaksono, S. T., Nikmah, H., Haryanto, H., Wardhana, A. G. S., Prakoso, A., Mujiburrosyid, A., Maulana, A., Gianfranco, E., Ihsan, H., Widagda, I. C., Febrada, M. H., Ariawan, M. E. W., Darajat, M. I., Alifan, M. M., Sanjaya, M. R., ... Raja, R. (2022). Teknologi Pembuatan Pakan Konsentrat Sapi Potong Sesuai Standar Nasional Indonesia (SNI) Berbasis Limbah Pertanian. *Sewagati*, 6(5). <https://doi.org/10.12962/j26139960.v6i5.398>

Deformation Resistance of Stone Mastic Asphalt Mixtures with Fiber Mesh Added Materials

Bulgis^{1,*}, Salim¹, Yogi Nauvally¹, Muh. Riyan¹,

¹ Department of Civil Engineering, Universitas Muslim Indonesia, Makassar, Indonesia

* Corresponding Author E-mail: bulgis.bulgis@umi.ac.id

Abstract

Road pavement deformation is a major issue caused by excessive traffic loads, leading to reduced durability and decreased riding comfort. Stone Mastic Asphalt (SMA) is a hot mix asphalt designed to withstand heavy vehicle loads due to its gap-graded structure and high asphalt content. However, its performance can be further enhanced with stabilizing additives such as fibers. Among various synthetic fibers, fiber mesh is a cost-effective material that can improve the mechanical properties of SMA. This study aims to analyze the effect of fiber mesh as an additive on the deformation resistance of SMA mixtures. A laboratory experimental approach was conducted by preparing SMA samples incorporating fiber mesh at a content of 0.3% of the total mixture weight and a fiber length of 0.36 cm. The deformation resistance of the samples was evaluated using a wheel tracking test to assess deformation depth, dynamic stability, and deformation rate. The results show that the addition of fiber mesh significantly reduces deformation in SMA mixtures compared to those without fiber mesh. The fiber-reinforced SMA exhibited higher dynamic stability and a lower deformation rate, indicating improved resistance to rutting and long-term durability. These findings suggest that fiber mesh is an effective additive for enhancing SMA performance, making it a promising solution for improving pavement lifespan and reducing maintenance needs.

Keywords:

Deformation; Fiber Mesh; Split Mastic Asphalt

1. INTRODUCTION

Stone Mastic Asphalt (SMA) mixture is designed with a gap-graded aggregate structure, predominantly composed of coarse aggregates, which play a crucial role in forming a stable and efficient framework for load distribution. This rigid frame structure allows SMA to effectively distribute loads from the surface down to the underlying layers, minimizing the potential for permanent deformation such as rutting and cracking (Bieliatynskyi et al., 2024; , Valdés et al., 2023). The effectiveness of SMA in load distribution can be attributed to its distinct compositional properties. SMA typically has a higher percentage of coarse aggregate compared to regular asphalt mixtures, creating a strong interlocking framework. This framework minimizes voids and improves the material's resistance to both permanent deformation and fatigue loading (Valdés et al., 2023; , Shaffie et al., 2023). Additionally, the presence of stabilizing additives, often in the form of fibers (natural and synthetic), further enhances the mechanical properties and moisture resistance of the mixture. Such additives play a crucial role in preventing the drain-down of asphalt mastic, which is particularly important in maintaining the integrity of the mix under varying environmental conditions (Alnadish et al., 2023; , Al-Saadi et al., 2023). This unique aggregate arrangement enhances the mixture's ability to resist deformation and rutting, making it highly suitable for high-traffic roads and heavy-load applications. The coarse aggregates in SMA are tightly interlocked, providing mechanical stability, while the voids between them are filled with a mastic-rich binder. This mastic consists of a combination of fine fillers, fibers, and polymers, which contribute to the durability and flexibility of the asphalt mixture. The relatively high asphalt content in SMA, as noted by Affandi (2010), results in a thick asphalt film that improves the mixture's resistance to fatigue and moisture damage. Additionally, the inclusion of fibers helps prevent asphalt binder drainage during mixing and placement, ensuring uniform distribution throughout the mixture. As a result, SMA

offers superior performance in terms of long-term durability, skid resistance, and reduced maintenance costs compared to conventional asphalt mixtures.

The correlation between increasing traffic volume and the resultant effects on asphalt pavement integrity, particularly through overload, is well-documented in road engineering literature. High traffic loads directly contribute to the deformation of asphalt surfaces, primarily manifesting as rutting, which is a critical failure mode resulting from repeated vehicle loading. This occurrence is emphasized by several studies that illustrate how excessive loads lead to deterioration in pavement quality (Aman et al., 2024; Albayati, 2023). As specified in the literature, heavy axle loads are a significant factor contributing to the fatigue life reduction of asphalt pavements, which are subjected to cyclical stress over time (Zhang et al., 2024). Moreover, Aman et al. discuss how permanent deformation, or rutting, is a prevalent issue in flexible pavements attributable to repetitive traffic loads, highlighting the necessity of using modified mixtures to mitigate these failures (Aman et al., 2024). This is complemented by studies indicating that inadequately designed asphalt mixtures and insufficient compaction during the construction phase exacerbate rutting, particularly in warm climates (Vámos & Szendefy, 2024; Taher et al., 2024). For instance, high temperatures coupled with increased traffic can soften the asphalt binder, thereby intensifying the risk of deformation under load (Vámos & Szendefy, 2024).

Deformation is a change in the shape, dimensions, and position of a material, whether part of nature or man-made, on a time and space scale (Sukmawaty, 2018). Deformation is an important deterioration of pavement conditions because it affects the quality of traffic comfort (roughness, puddles of water, which affect surface roughness) and can reflect damage to the pavement structure. One of the advantages of the SMA mixture (Błazejowski, 2016) is its high resistance to deformation as a result of the large coarse aggregate content and the formation of a strong aggregate framework. Past studies have demonstrated that the coarse aggregates in SMA typically comprise 70-80% of the mixture by weight and contribute significantly to the robust mechanical interlock essential for resisting permanent deformation and rutting under load (Jivitha et al., 2024; Sihombing et al., 2023; Kumar, 2023). The effectiveness of the stone-on-stone contact that occurs within the coarse aggregate skeleton prevents lateral displacement during stress application, which is critical for maintaining long-term pavement integrity (Shaffie et al., 2023; Raj & Ramesh, 2024). However, the SMA mixture contains a high asphalt content, so an additional material (additive) is needed that can stabilize and give strength. One additional material that can be used is fiber (Aminin, 2020). Fiber is an additional material that functions to absorb some of the asphalt. Fiber consists of pieces of components that form a complete elongated network. Fiber can be classified into two types, namely natural fibers and synthetic fibers (man-made fibers). Synthetic fibers can be produced cheaply in large quantities, one of which is fiber mesh.

1.1 Research Purposes

This research aims to analyze the influence of Fiber Mesh as an additional material on the performance characteristics of Stone Mastic Asphalt (SMA) mixtures, particularly in terms of their resistance to deformation. The study focuses on evaluating how the incorporation of Fiber Mesh affects key parameters such as deformation resistance, dynamic stability, and the rate of deformation under varying conditions. By examining these aspects, the research seeks to determine the extent to which Fiber Mesh enhances the structural integrity and durability of SMA mixtures, potentially contributing to improved road pavement performance and longevity.

1.2 Study Literature

Research on the use of cellulose fiber as an added material has been carried out, including research using Viatop66 (Abdillah et al., 2018), showing that the addition of Viatop66 cellulose fiber in SMA mixtures has an optimum limit of around 0.3%–0.4% of the total weight of the mixture. This is in accordance with what has been determined by SNI for the addition of additional ingredients in the form of cellulose fiber, namely 0.3% of the total weight of the mixture. The results of this research are a reference for determining the levels of added materials with different materials, namely fibermesh. Research Asbuton (LGA 50/25) (Suaryana, 2016) can behave as a stabilizer like cellulose fiber. LGA functions as a stabilizer, presumably because there is no

asphalt mobilization in LGA as a whole, and the relatively lower penetration rate of asphalt results in increased binder viscosity. In terms of resistance to fatigue, SMA with a cellulose stabilizer and SMA with an asphalt stabilizer have relatively the same performance. The fatigue performance of SMA blends and SMAB blends proves that SMAB is not only resistant to permanent deformation, as shown in the stability dynamic values, but also has sufficient flexibility, as shown in the relationship between strain and number of cycles. Researchers used the results of this study as a reference for SMA mixtures based on deformation testing with different materials. Research carried out (Alifuddin & Arifin, 2020) using asbestos fiber as an added material showed that the percentage value of the cellulose fiber (asbestos) added material used in the Split Mastic Asphalt (SMA) mixture met the optimum fiber content percentage, namely 2.81%. The percentage of cellulose fiber added to the Split Mastic Asphalt (SMA) mixture can increase the characteristic values of the asphalt concrete mixture. Researchers used the results of this research as a reference for SMA mixtures with different added materials. Research carried out in (Tahir .2011, n.d.) used rice bran as an added material. The results of the examination and analysis of the characteristics of the Split Mastic Asphalt (SMA) mixture using cellulose-added material (rice bran) show an increase in the performance of the asphalt concrete mixture. This research is a reference on SMA mixtures with different added ingredients and different testing methods.

2. METHODS

2.1 Making Test Objects

The materials used in this research were previously examined in the laboratory to obtain materials that meet the requirements for road work materials (Direktorat Jenderal Bina Marga, 2018). The asphalt content used is the optimum asphalt content, then mixed with fiber mesh as an additive to the asphalt. The fiber mesh used in this research is fiber mesh with a length of 0.36 cm and a content of 0.3% of the mixture weight; this is based on the best value from previous research (Bastari & Bulgis, 2023), (Bulgis & Salim, 2023).



Figure 1. Fibermesh after cutting

2.2 Deformation Testing

Sample testing was carried out after all the ingredients were mixed and then stirred thoroughly until it reached a temperature of $\pm 150^{\circ}\text{C}$. Next, the mixture is put into a mold measuring $30 \times 30 \times 5$ cm, and the mixture is compacted in 50 strokes. Next, the test object is cooled to room temperature, then removed from the mold and left at room temperature for 24 hours before being tested. Testing of test objects to obtain deformation values using the wheel tracking tool.



Figure 2. Whell Tracking Machine

3. RESULT AND DISCUSSION

3.1 SMA Pavement Mixture Composition

Before mixing the ingredients, check the materials to be used. The types of materials examined were aggregate CS 2-3, CS 1-2, CS 0.5-1, and stone ash from Bili-Bili Makassar, while the asphalt used was Pertamina penetrasi 60/70 asphalt. Based on the inspection results, it shows that the above materials have met the required specifications. (Bina Marga). Next, determine the aggregate composition based on the results of the sieve analysis. The aggregate composition obtained from the results of combining the aggregates is shown in Table 1.

Table 1. Aggregate Composition

Sieve of Number	% Passing CS 2 - 3	% Passing CS 1 - 2	% Passing CS 0,5 - 1	% Passing Stone Ash	CS 2 - 3	CS 1 - 2	CS 0,5 - 1	Stone Ash	Total Aggregate	Specification		
					31%	26%	23%	20%			-	
25 (1")	100	100	100	100	31	26	23	20	100	100	-	100
19,1 (3/4")	83.93	100	100	100	26.02	26.00	23.00	20.00	95.02	90	-	100
12,7 (1/2")	27.47	67.38	100	100	8.51	17.52	23.00	20.00	69.03	50	-	88
9,52 (3/8")	0.30	36.25	56.34	100	0.09	9.43	12.96	20.00	42.48	25	-	60
No. 4	0	0.30	17.14	100	0	0.08	3.94	20.00	24.02	20	-	28
No. 8	0	0	0.27	99.60	0	0	0.06	19.92	19.98	16	-	24
No. 200	0	0	0	40.06	0	0	0.00	8.01	8.01	8	-	11

The results of the aggregate composition combining using the trial and error method determined that the aggregate composition was Crushed Stone (CS) (2–3) 31%, CS (1-2) 26%, CS (0.5–1) 23%, and Stone Ash 20%.

3.2 Determination of Optimum Asphalt Content

Next, the optimal asphalt content is determined from the plan asphalt content. The optimal asphalt content in a mixture influences the characteristics of the asphalt mixture, such as density, void in mix (VIM), void in material aggregates (VMA), VFA, stability, flow, and Marshall quotient.

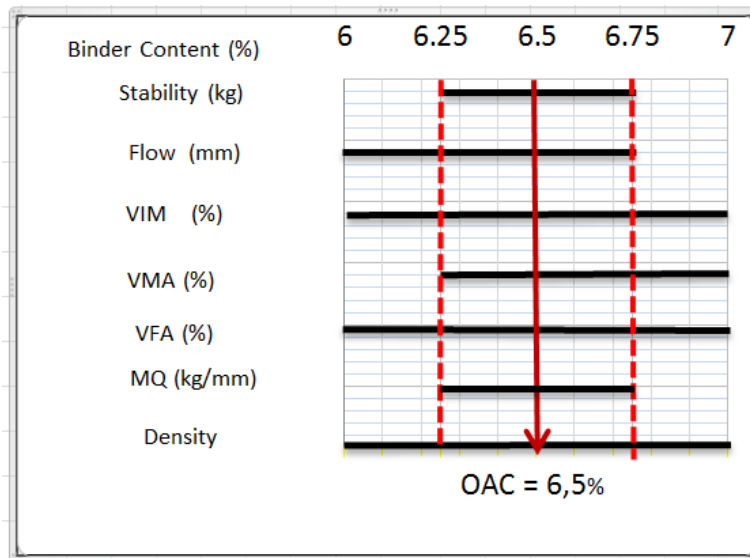


Figure 3. Optimum Asphalt Content (OAC)

Figure 3. regarding determining the OAC value using the barchart method, shows the relationship between asphalt content and mixture characteristics using the middle value on the graph that meets the characteristics of the Marshall Test. Starting from the minimum value obtained, namely 6%, and the maximum value obtained, namely 7%, Characteristics that meet specifications start at 6.25%, 6.5%, and 6.75%, so that the OAC determination is obtained at 6.5%.

The optimum asphalt content (OAC) value will be used in planning SMA mixtures with variations in the added material of Cellulose Fiber Mesh with variations in the added material content of 0%, 0.1%, 0.2%, 0.3%, and 0.4% of the total weight of the mixture with a length of 0.36 cm, 0.72 cm, 1.08 cm, 1.44 cm, and 1.80 cm. From the results of the analysis, determining the optimum fiber mesh content is also the same as determining the length, namely, by reference to the stability value, the highest marshall quotient of each grade with the minimum flow of all existing fiber mesh grades. The highest stability and marshall quotient values have a content of 0.3% and a length of 0.36 cm of 737.916 kg and 217.159 kg/mm, respectively, with a minimum flow value of 3.4 mm.

3.3 Deformation Test Results (Wheel Tracking)

Deformation Test Results (Wheel Tracking) This test was carried out to see the deformation resistance performance of the mixture based on the optimal asphalt content (KAO) with a content of 6.5%, a fiber mesh content of 0.3%, and a length of 0.36 cm. A review of three Wheel Tracking test parameters was carried out, namely groove depth (deformation), deformation rate (RD), and dynamic stability (DS). The following describes the wheel tracking test results shown in Table 2 and Table 3.

Table 3. Wheel Tracking Test Results for SMA Pavement without Fiber mesh

Time/Minutes	Number of cycles	30°C SMA Pavement Without Fiber mesh	Unit
0	0	0	mm
1	42	0.90	mm
5	210	1.10	mm
10	420	1.30	mm
15	630	1.70	mm
30	1260	3.10	mm
45	1890	3.40	mm
60	2520	3.90	mm
Total Deformation (D0)		2.200	mm
Dynamic Stability (DS)		2520	passes/mm
Deformation Rate (RD)		0.033	mm/minutes

Table 4. Wheel Tracking Test Results for SMA Pavement with Fiber mesh

Time/Minutes	Number of cycles	30°C SMA Pavement With Fiber mesh	Unit
0	0	0	mm
1	42	0.90	mm
5	210	0.98	mm
10	420	1.10	mm
15	630	1.30	mm
30	1260	1.40	mm
45	1890	1.50	mm
60	2520	1.70	mm
Total Deformation (D0)		1.269	mm
Dynamic Stability (DS)		6300	passes/mm
Deformation Rate (RD)		0.013	mm/minutes

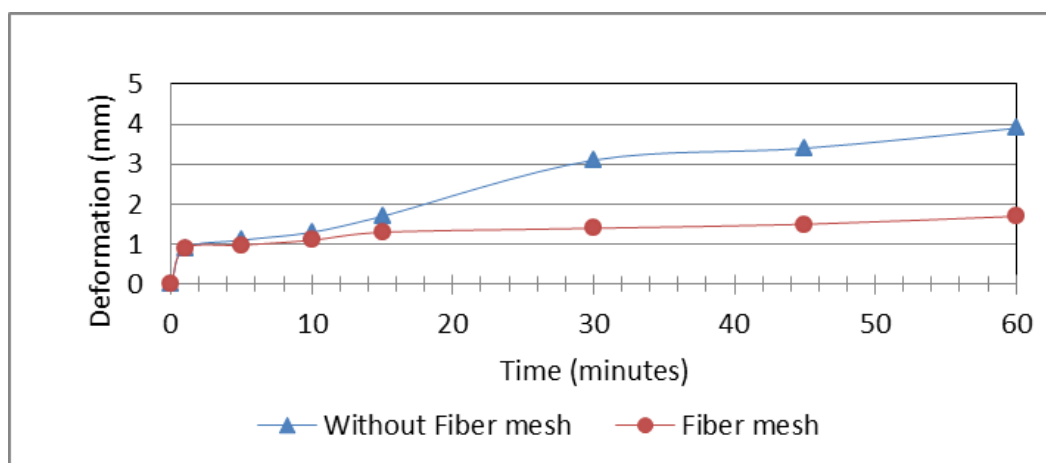


Figure 4. Comparison of Deformation of SMA Mixtures Without Fiber Mesh and Fiber Mesh

Based on Figure 4. and the comparison of the deformation of the SMA mixture without added fiber mesh and with fiber mesh, it is observed that changes in deformation tend to decrease as time increases. The mixture without fiber mesh has a high deformation change, namely 3.90 mm, up to 60 minutes, and the mixture using fiber mesh has a low change, with a value of 1.70 mm up to 60 minutes.

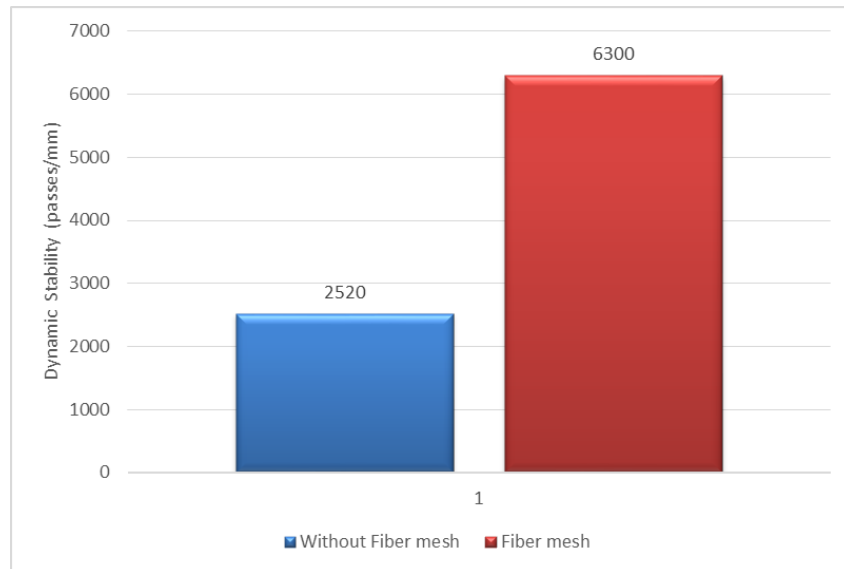


Figure 5. Dynamic Stability of SMA Mixtures without Fiber mesh and Fiber mesh

Figure 5 shows that the dynamic stability of the SMA mixture without fiber mesh and the fiber mesh observed in the mixture with fiber mesh obtained the highest dynamic stability of 6300 passes/mm. Meanwhile, the lowest dynamic stability was shown in the mixture without fiber mesh at 2520 passes/mm.

The dynamic stability value is inversely proportional to the amount of deformation that occurs; namely, the dynamic stability value is greater in the mixture using fiber mesh. The greater it indicates that the dynamic stability of the mixture decreases, so that the deformation resistance decreases.

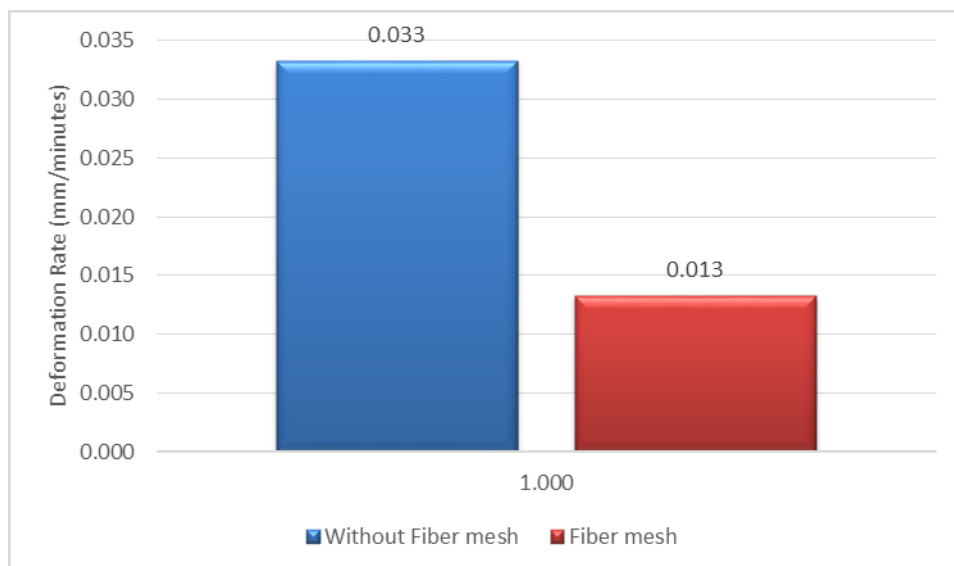


Figure 6. Deformation rate of SMA mixture without fiber mesh and fiber mesh

Figure 6 shows the amount of deformation that occurs in the SMA mixture each time. In the SMA mixture using cellulose fiber mesh, the lowest deformation rate was obtained with a value of 0.013 mm/minute, while the mixture without fiber mesh was 0.033 mm/minute.

The lower deformation rate obtained in mixtures that use fiber mesh indicates that the mixture has good stability and is resistant to deformation.

The results of this study indicate that the addition of fiber mesh significantly improves the deformation resistance of Stone Mastic Asphalt (SMA) mixtures. The comparison between SMA mixtures with and without fiber mesh shows a noticeable reduction in deformation, with the fiber mesh-enhanced mixture demonstrating superior resistance to rutting. This aligns with previous studies that highlight the effectiveness of synthetic fibers in enhancing the structural integrity of asphalt mixtures by improving their load distribution and reducing susceptibility to permanent deformation. The effectiveness of synthetic fibers in enhancing the structural integrity of asphalt mixtures is well-documented in the literature. Fibers, such as basalt, polyester, and polypropylene, have been shown to significantly improve the load distribution capabilities of asphalt mixtures, leading to reduced permanent deformation and enhanced durability (Guo et al., 2023; Jiu et al., 2023; Jia et al., 2023). Specific studies have demonstrated that the incorporation of various types of fibers contributes to increased dynamic stability and fatigue resistance, which are vital for the performance of asphalt roads under traffic loads and environmental stresses (Taher et al., 2023; Jiu et al., 2023). The reduction in deformation can be attributed to the ability of fiber mesh to reinforce the asphalt mastic, creating a more cohesive and stable matrix that resists the stresses imposed by traffic loads.

Furthermore, the dynamic stability results reinforce the role of fiber mesh in enhancing the long-term durability of SMA mixtures. The significantly higher dynamic stability values observed in fiber mesh-reinforced SMA indicate that these mixtures can withstand more load repetitions before experiencing substantial deformation. Research has shown that fibers act as reinforcements within asphalt mixtures, significantly improving resistance to permanent deformation. For instance, the study by Ji et al. reveals that basalt fibers, when incorporated into SMA mixtures, create a robust three-dimensional network that enhances the mechanical properties, thereby increasing overall durability and dynamic stability (Ji et al., 2024). Similarly, Alifuddin et al. highlight that the addition of fibers increases the stiffness, toughness, and fatigue resistance of asphalt mixtures, thereby reducing maintenance costs and extending service life (Alifuddin et al., 2024). Furthermore, studies involving synthetic fibers have documented improvements in rutting resistance, where mixtures enriched with these fibers could withstand higher loads before exhibiting permanent deformation (Aman et al., 2024; , Jia et al., 2023). This is an important finding, as high dynamic stability is a critical parameter for road pavements subjected to heavy traffic. The increased dynamic stability observed in this study aligns with previous research on cellulose and synthetic fiber additives, which have been shown to enhance the structural performance of asphalt mixtures by preventing binder drain-down and improving cohesion.

The lower deformation rate recorded in fiber mesh-reinforced SMA mixtures also suggests improved resistance to environmental factors such as temperature fluctuations and moisture exposure. In regions with high temperatures, asphalt mixtures are prone to softening, which can lead to accelerated rutting. The softening of asphalt at elevated temperatures is primarily due to its viscoelastic properties, making it susceptible to deformation under repeated traffic loading conditions (Akkenzheyeva et al., 2024; ,Mahan et al., 2023). However, the addition of fiber mesh appears to mitigate this issue by enhancing the internal structure of the SMA mixture, making it more resistant to plastic deformation. This finding is consistent with prior studies that have demonstrated the role of fibers in improving the viscoelastic properties of asphalt binders, thereby increasing the mixture's ability to recover from deformation under repeated loading.

In addition to improving mechanical performance, the use of fiber mesh in SMA mixtures presents potential cost and sustainability benefits. The reduction in deformation and rutting implies longer pavement lifespan and reduced maintenance costs, which is particularly beneficial for heavily trafficked roads. Moreover, fiber mesh is a relatively affordable and widely available material, making it a practical solution for asphalt modification (Alnadish et al., 2023). Future research could explore the use of alternative fiber materials, including recycled or natural fibers, to further enhance the sustainability of SMA mixtures while maintaining their high-performance characteristics.

4. CONCLUSIONS

Split Mastic Asphalt (SMA) pavement mixture with an optimum asphalt content of 6.5% using synthetic cellulose fiber mesh with a content of 0.3% and a length of 0.36 cm, it can be concluded that the comparison of deformation without and using fiber mesh, namely the occurrence of deformation changes, has decreased with the presence of fiber mesh. This shows better deformation resistance than without using fiber mesh.

The results of this study demonstrate that the addition of fiber mesh significantly enhances the deformation resistance of Stone Mastic Asphalt (SMA) mixtures. The comparison between SMA mixtures with and without fiber mesh shows a notable reduction in deformation, a higher dynamic stability, and a lower deformation rate in mixtures containing fiber mesh. These findings indicate that fiber mesh effectively reinforces the asphalt matrix, improving load distribution and increasing the pavement's ability to withstand repeated traffic loads.

Furthermore, the increased dynamic stability and reduced deformation rate suggest that fiber mesh-reinforced SMA mixtures exhibit superior durability and resistance to environmental stressors such as high temperatures and heavy axle loads. The findings align with previous research on fiber additives in asphalt, confirming that fiber mesh enhances the structural integrity of SMA mixtures by reducing rutting and extending pavement lifespan. The economic and practical advantages of fiber mesh, including its cost-effectiveness and ease of application, further support its potential as a viable alternative to traditional stabilizing agents.

In conclusion, this study provides strong evidence that fiber mesh is a beneficial additive for SMA mixtures, offering improved performance in terms of deformation resistance, stability, and durability. Future research should focus on field applications and long-term performance evaluations to validate these laboratory findings in real-world road conditions. Additionally, exploring the use of alternative fiber materials, including recycled or natural fibers, could further enhance the sustainability and effectiveness of SMA mixtures in pavement construction.

REFERENCES

- Abdillah, A. F., Pradani, N., & Batti, J. F. (2018). Pengaruh Penggunaan Bahan Tambah VIATOP66 pada Campuran Stone Matrix Asphalt Terhadap Titik Lembek Aspal dan Sifat Drain Down Campuran. *Jurnal HPJI*, 4(1), 49–58.
- Affandi, F. (2010). Pengaruh Asbuton Semi Ekstraksi pada Campuran Stone Mastic Asphalt. *Jurnal Jalan-Jembatan*, 27(1), 1–13.
- Akkenzheyeva, A., Haritonovs, V., Bussurmanova, A., Merijs-Meri, R., Imanbayev, Y., Serikbayeva, A., ... & Turkmenbayeva, M. (2024). The use of rubber-polymer composites in bitumen modification for the disposal of rubber and polymer waste. *Polymers*, 16(22), 3177. <https://doi.org/10.3390/polym16223177>
- Al-Saadi, I., Tayh, S., Jasim, A., & Yousif, R. (2023). The use of natural fibers in stone mastic asphalt mixtures: a review of the literature. *Archives of Civil Engineering*. <https://doi.org/10.24425/ace.2023.146085>
- Albayati, A. (2023). A review of rutting in asphalt concrete pavement. *Open Engineering*, 13(1).

<https://doi.org/10.1515/eng-2022-0463>

- Alifuddin, A., Massara, A., Muhammad, V., & Mardin, N. (2024). Optimizing the use of palm fiber to increase stability and deformation resistance in asphalt concrete mixes. *Intek Jurnal Penelitian*, 11(1), 13-25. <https://doi.org/10.31963/intek.v11i1.4745>
- Alifuddin, A., & Arifin, W. (2020). Analisis Durabilitas Campuran Split Mastic Asphalt (SMA) Terhadap Penggunaan Serat Selulosa (Serat Asbes). *Jurnal Teknik Sipil MACCA*, 5(2), 67–78.
- Alnadish, A., Singh, N., & Alawag, A. (2023). Applications of synthetic, natural, and waste fibers in asphalt mixtures: a citation-based review. *Polymers*, 15(4), 1004. <https://doi.org/10.3390/polym15041004>
- Aman, M., Musa, N., Bujang, H., Shahadan, Z., Taher, M., Rohani, M., ... & Arumugam, T. (2024). Assessment of permanent deformation on asphalt mixtures incorporating forta-fi fibre as additive material. *Iop Conference Series Earth and Environmental Science*, 1347(1), 012049. <https://doi.org/10.1088/1755-1315/1347/1/012049>
- Aminin, R. (2020). Karakteristik Marshall Campuran Split Mastic Asphalt (SMA) Dengan Penambahan Selulosa Serat Kapuk. *Repository Universitas Jember, September 2020*, 72–82.
- Bastari, R., & Bulgis, B. (2023). KARAKTERISTIK MARSHALL CAMPURAN STONE MASTIC ASPHALT DENGAN PENGGUNAAN FIBER MESH SEBAGAI BAHAN TAMBAH. 6(4), 1103–1116.
- Bieliatynskiy, A., Yang, S., Pershakov, V., Shao, M., & Ta, M. (2024). Features of the structure and properties of stone mastic asphalt. *Materialwissenschaft Und Werkstofftechnik*, 55(7), 986-994. <https://doi.org/10.1002/mawe.202300181>
- Błazejowski, K. (2016). Stone matrix asphalt: Theory and practice. In *Stone Matrix Asphalt: Theory and Practice*.
- Bulgis, B., & Salim, S. (2023). Selulosa Fiber Mesh Bahan Tambah Campuran Stone Mastic Asphalt. *Jurnal Arsip Rekayasa Sipil Dan Perencanaan*, 6(3), 147–157. <https://doi.org/10.24815/jarsp.v6i3.31218>
- Direktorat Jenderal Bina Marga. (2018). Spesifikasi Umum Untuk Pekerjaan Konstruksi Jalan dan Jembatan. In *Edaran Dirjen Bina Marga Nomor 02/SE/Db/2018* (Issue September).
- Guo, Y., Tataranni, P., & Sangiorgi, C. (2023). The use of fibres in asphalt mixtures: a state of the art review. *Construction and Building Materials*, 390, 131754. <https://doi.org/10.1016/j.conbuildmat.2023.131754>
- Jia, H., Sheng, Y., Guo, P., Underwood, B., Chen, H., Kim, Y., ... & Ma, Q. (2023). Effect of synthetic fibers on the mechanical performance of asphalt mixture: a review. *Journal of Traffic and Transportation Engineering (English Edition)*, 10(3), 331-348. <https://doi.org/10.1016/j.jtte.2023.02.002>
- Jiu, X., Wang, Y., Wu, Z., Xiao, P., & Kang, A. (2023). High-temperature performance evaluation of asphalt mixtures by adding short-chopped basalt fiber. *Buildings*, 13(2), 370. <https://doi.org/10.3390/buildings13020370>
- Jivitha, N., Ramesh, A., Ramayya, V., & Kumar, M. (2024). Synergistic improvement of stone matrix asphalt mixtures incorporating reclaimed asphalt aggregates and warm mix additives using multivariate analysis.. <https://doi.org/10.21203/rs.3.rs-5414341/v1>
- Kumar, G. (2023). Performance of stone matrix asphalt modified with crumb rubber and fibres. *Jordan Journal of Civil Engineering*, 17(4). <https://doi.org/10.14525/jjce.v17i4.08>
- Mahan, H., Ajam, H., & Jassim, H. (2023). Enhancing marshall properties through the integration of waste plastic water bottles in dry process asphalt production. *Mathematical Modelling and Engineering Problems*, 10(5), 1817-1823. <https://doi.org/10.18280/mmep.100534>
- Raj, N. and Ramesh, A. (2024). Development of sustainable pavement: an experimental study of stone mastic asphalt prepared with warm mix additives and reclaimed asphalt pavement. *Iop Conference Series Earth and Environmental Science*, 1326(1), 012082. <https://doi.org/10.1088/1755-1315/1326/1/012082>
- Shaffie, E., Shiong, F., Ismail, N., Ahmad, J., Arshad, A., & Ismail, M. (2023). Statistical analysis of stone mastic asphalt containing steel fiber. *Iop Conference Series Earth and Environmental Science*, 1151(1), 012040. <https://doi.org/10.1088/1755-1315/1151/1/012040>
- Sihombing, A., Utami, R., Somantri, A., Febriansya, A., Sihombing, R., & Mulyadi, A. (2023). Stone matrix asphalt performance with glycerin pitch as asphalt binder extender. *Periodica Polytechnica Civil*

- Engineering. <https://doi.org/10.3311/ppci.21817>
- Suaryana, N. (2016). Performance evaluation of stone matrix asphalt using Indonesian natural rock asphalt as stabilizer. *International Journal of Pavement Research and Technology*, 9(5), 387–392. <https://doi.org/10.1016/j.ijprt.2016.09.007>
- Sukmawaty, D. (2018). Analisis Deformasi Tanah Lunak Terhadap Perkuatan Geogrid Menggunakan Metode Elemen Hingga. *Siimo Engineering: Journal Teknik Sipil*, 2(2003), 1–8. <http://jurnal.unismuhpalu.ac.id/index.php/SiimoEngineering/article/view/443>
- Taher, M., Aman, M., & Bujang, H. (2024). The influence of basalt aggregate on the mechanical performance of hot mix asphalt (hma) mixtures. *Journal of Advanced Research in Applied Mechanics*, 121(1), 1-12. <https://doi.org/10.37934/aram.121.1.112>
- Taher, M., Aman, M., Bujang, H., & Rusli, H. (2023). Stiffness evaluation of forta fibre reinforced asphalt concrete (frac) mixture under different pulse repetition load. *Iop Conference Series Earth and Environmental Science*, 1205(1), 012066. <https://doi.org/10.1088/1755-1315/1205/1/012066>
- Tahir .2011. (n.d.). Kinerja campuran. *Kinerja Campuran Split Mastic Asphalt (SMA) Yang Menggunakan Serat Selulosa Alami Dedak Padi*.
- Valdés, G., Calabi-Floody, A., Mignolet-Garrido, C., & Díaz-Montecinos, C. (2023). Effect of a new additive based on textile fibres from end-of-life tyres (elt) on the mechanical properties of stone mastic asphalt. *Polymers*, 15(7), 1705. <https://doi.org/10.3390/polym15071705>
- Vámos, M. and Szendefy, J. (2024). Temperature effects on traffic load-induced accumulating strains in flexible pavement structures. *International Journal of Pavement Research and Technology*. <https://doi.org/10.1007/s42947-024-00466-4>
- Zhang, W., Han, W., Jiang, W., Cui, T., Wang, S., Yang, F., ... & Wei, J. (2024). Fatigue damage in asphalt pavement based on axle load spectrum and seasonal temperature. *Coatings*, 14(7), 882. <https://doi.org/10.3390/coatings14070882>

Pre-Design and Environmental Impact Analysis of Methanol Plant from Natural Gas with Dielectric Barrier Discharge Reactor

Jansen Briano ^{1,*}, Kornelius S. Tanuwidjaja ¹, Yosia G. Kurniawan ¹, Meyland ¹, Samuel P. Aletheia ¹

¹ Chemical and Food Processing, Calvin Institute of Technology, Jakarta, Indonesia

* Corresponding Author E-mail: jbriano.work@gmail.com

Abstract

In Indonesia, the demand for methanol reaches 1.1 million tons per year, with the majority being fulfilled through imports. The formaldehyde industry is the primary consumer, using 80% of the total methanol consumption. Increasing domestic methanol production has become crucial due to dependency on imports and the presence of only one producer with a capacity of 660,000 tons per year. The preliminary design of a low-emission methanol plant is a first step toward a more environmentally friendly methanol industry in Indonesia, aiming to reduce carbon emissions and dependence on fossil fuels. Methanol production at this plant results in the lowest possible carbon emissions, using raw materials such as methane gas, purified water, and helium. The methane gas is sourced from pure liquified natural gas (LNG) from PT Badak NGL, which has been purified from CO₂ and H₂S under operating conditions of -162°C and 1 bar pressure. Meanwhile, the purified water is obtained through seawater desalination processes. The reaction between methane and purified water occurs in a dielectric barrier discharge (DBD) reactor at 1 bar pressure, with helium as the inert gas. The plant's production capacity reaches 500,000 tons per year, with a purity level of 99.95% and zero greenhouse gas emissions. To achieve profitability comparable to conventional methanol, a minimum methanol selling price of \$970/ton is required. When the carbon credit price is \$1200/tCO₂, the methanol produced by this plant will be more profitable for investors compared to conventional methanol production or methanol production using carbon capture and utilization technology.

Keywords:

Dielectric Barrier Discharge (DBD); Direct Conversion; Methanol Production; Low Carbon Emission; Plasma Reactor

1. INTRODUCTION

East Kalimantan, Indonesia, stands out as a prime location for establishing chemical production facilities, particularly for liquefied natural gas (LNG) and methanol, due to its substantial gas reserves in fields such as Badak, Nilam, and Semberah. The Bontang LNG plant, one of the largest globally, has been operational since 1977 and supplies LNG to major markets like Japan, South Korea, and Taiwan. This facility's modern infrastructure, combined with its proximity to offshore reserves, makes it a reliable and strategic site for large-scale LNG production and export. East Kalimantan's location further enhances its role as a key export hub to major Asian consumers, bolstered by government support aimed at prioritizing industrial development in the region (Hydrocarbons Technology; ERIA, 2021; Indonesia Investments, 2016).

Methanol production is increasingly relevant to Indonesia's industrial and energy strategies due to rising global demand, projected to reach 500 million tons by 2050 (IRENA, 2021). Currently, Indonesia's methanol demand is around 1.1 million tons annually, with over 80% met through imports (Maulana, 2021). Methanol has extensive applications across Indonesian industries, including fuel production, chemical manufacturing, solvents, and cosmetics. Importantly, methanol as a fuel helps reduce emissions of pollutants such as carbon monoxide (CO), hydrocarbons (HC), and nitrogen oxides (NO_x) in combustion engines (Albana). Methanol is also integral to Indonesia's biodiesel initiatives (B30), a program that saved the country \$4.54 billion in foreign exchange and cut CO₂ emissions by 25 million tons in 2021, with future plans to increase blending rates to B40 and B50 driving additional domestic demand for methanol (Ministry of Energy and Mineral Resources, 2021).

doi http://dx.doi.org/10.51557/pt_jiit.v10i1.2950

article history: Received October 24, 2024; Received in revised from March 01, 2025; Accepted March 02, 2025;
Available online March 25, 2025.

This is an open access article under the [CC-BY-SA](https://creativecommons.org/licenses/by-sa/4.0/) license



LNG serves as a cleaner alternative to coal for methanol production in East Kalimantan, supporting Indonesia's climate goals and aligning with commitments under the Paris Agreement and COP28. Utilizing LNG, alongside advanced technologies such as the Dielectric Barrier Discharge (DBD) reactor for methane-to-methanol conversion, holds potential to reduce emissions. DBD reactors operate at lower temperatures and avoid intermediate steps like syngas production, thus reducing both energy consumption and carbon emissions. This aligns with Indonesia's Nationally Determined Contributions (NDCs), underscoring the country's proactive stance in global climate action and strengthening its energy security by advancing cleaner industrial practices.

However, the use of LNG for methanol production presents notable challenges. Methane leakage, which can occur during extraction, processing, and transport, contributes to greenhouse gas emissions, offsetting some environmental benefits of LNG (Kourkoumpas et al., 2018). While technologies like the DBD reactor show promise for low-emission methanol production, maintaining optimal conditions is complex and energy-intensive, often requiring a renewable energy supply to fully realize CO₂ emissions reductions (Román-Leshkov & Dumesic, 2014). Additionally, the infrastructure needed for LNG production, storage, and transport is costly, and lapses in maintenance can exacerbate methane leakage, potentially undermining emission reduction goals (Yang et al., 2019). Addressing these challenges demands continuous innovation and robust methane management strategies to ensure that LNG-based methanol production aligns with Indonesia's climate objectives.

Methanol production from LNG not only offers a cleaner combustion profile but also allows flexibility in supply chain diversification, enhancing energy security and price stability (Yusuf, 2023). As Indonesia aims to reduce carbon emissions and transition towards cleaner energy, LNG-based methanol production could serve as a bridge to a sustainable energy future, offsetting some reliance on coal power and reducing methanol import dependency. Currently, Indonesia Kaltim Methanol Industri, the primary domestic producer, has an annual capacity of 660,000 tons, indicating potential for expansion (Pardero et al., 2022).

This research aims to design a sustainable methanol production plant in East Kalimantan, leveraging local natural gas reserves. The study will evaluate the potential of DBD technology for methanol production, simulate the production process, and analyze carbon emissions, energy consumption, and economic viability, using metrics such as NPV, IRR, and payback period. This approach supports Indonesia's economic growth and climate commitments by advancing cleaner methanol production methods. Additionally, it aims to reduce reliance on methanol imports, bolstering key industries like biodiesel and chemical manufacturing while contributing to environmental sustainability.

2. RESEARCH METHODS

This study aims to analyze the feasibility of producing methanol directly from methane using a plasma-based conversion method. The research methodology includes a comprehensive literature review, process modeling and simulation, and an economic analysis to evaluate both the technical and financial viability of this production approach. By investigating key factors such as reaction mechanisms, process efficiency, and economic performance, this research contributes valuable insights into the potential for more sustainable and efficient methanol production technologies.

2.1 Literature Review

This literature review establishes the foundation for understanding the complex dynamics of direct methane-to-methanol conversion through plasma technology. In examining past research, emphasis was placed on identifying parameters critical to simulating this conversion and on addressing challenges inherent in the process. The review spans multiple areas, including reaction mechanisms, catalyst performance, plasma technology, separation techniques, and equipment design, to provide a comprehensive understanding of this emerging approach to methanol production.

Traditionally, methanol production has relied on syngas—a mixture of hydrogen (H₂) and carbon dioxide (CO₂) generated through the gasification of raw materials such as coal or biomass. This conventional method is energy-intensive and produces significant CO₂ emissions, which has led to the exploration of alternative feedstock and technologies that incorporate carbon capture or utilize H₂ generated via renewable-powered electrolysis. Despite these adaptations, methanol production via syngas remains energy-demanding, prompting recent studies to investigate direct methane-to-methanol conversion as a more energy-efficient approach.

Table 1 below compares conventional methanol production reactions with those involved in direct methane-to-methanol conversion. It is evident from these reactions that the energy required in conventional processes is generally higher due to the endothermic nature of the first step, highlighting a potential advantage of direct conversion methods in energy savings.

Table 1. Methanol Process Reactions (Al-Rowaili et al., 2022; Pröll & Lyngfelt, 2022; Li et al., 2021)

Conventional Methanol Production Reactions	Direct Methane to Methanol Production Reactions
CH ₄ (g) + H ₂ O(g) ⇌ CO(g) + 3H ₂ (g) ($\Delta H_{298K} = +206 \text{ kJ/mol}$)	CH ₄ + 1/2O ₂ ⇌ CH ₃ OH(g) ($\Delta H_{298K} = -126 \text{ kJ/mol}$)
CO(g) + H ₂ O(g) ⇌ CO ₂ (g) + H ₂ (g) ($\Delta H_{298K} = -41 \text{ kJ/mol}$)	CH ₄ + H ₂ O ⇌ CH ₃ OH + H·
CH ₄ (g) + 2H ₂ O(g) ⇌ CO ₂ (g) + 4H ₂ (g) ($\Delta H_{298K} = +165 \text{ kJ/mol}$)	CH ₄ + N ₂ O → CH ₃ OH + N ₂ ($\Delta H_{298K} = -159.0 \text{ kJ/mol}$)
CO ₂ (g) + 3H ₂ (g) ⇌ CH ₃ OH(g) + H ₂ O(g) ($\Delta H_{298K} = -49,16 \text{ kJ/mol}$)	
CO(g) + 2H ₂ (g) ⇌ CH ₃ OH(g) ($\Delta H_{298K} = -90,64 \text{ kJ/mol}$)	

One of the primary challenges in the direct conversion of methane to methanol lies in the thermodynamics. This process typically demands more energy to activate methane than is required to convert methanol to CO or CO₂, which has spurred research into low-energy and low-temperature conversion methods. Plasma-assisted conversion, particularly with Dielectric Barrier Discharge (DBD) reactors, emerges as a promising solution, as it provides the necessary energy to facilitate reactions under milder conditions than conventional thermal processes. Plasma reactors are advantageous in handling methane's high activation energy while minimizing methanol over-oxidation at high temperatures.

The role of catalysts and reactant compositions is also critical for optimizing conversion efficiency and reducing byproducts. Studies by Zakaria (2016) and Nandy (2022) underscore the importance of selectivity and efficiency in methane oxidation, while Li (2023) addresses the temperature sensitivity of methane as a key bottleneck in this process. Consequently, this study adopts a low-temperature plasma reactor to address these issues, aiming to enhance selectivity and reduce over-oxidation in methanol production.

A promising approach is the use of a non-thermal plasma reactor, particularly one utilizing DBD technology. Most prior studies have been limited to small-scale experiments, motivating this study to evaluate DBD performance on an industrial scale using DWSim simulation software. DWSim is selected for its open-source nature, making it accessible for academic research without the licensing fees associated with proprietary tools like Aspen Plus and CHEMCAD. Its accuracy in gas-phase reaction simulations has been validated in studies by Subramanian (2023) and Andreasen (2022) for applications such as hydrogen production and gas plant simulations. While DWSim does lack a developed library for plasma-specific reactions and cannot simulate plasma properties or radical ions—limitations that commercial software may overcome—it remains a versatile, cost-effective option for simulating heat exchangers, separation units, and reactors. Additionally, copper electrodes, known to enhance plasma production and conversion efficiency, are incorporated into this reactor design.

Tables 2 and 3 list the inlet flow and reactor operating conditions assumed in this study, informed by prior research including Bi et al., to provide a baseline for simulation.

Table 2. Inlet Conditions of DWSim Parameters

Flow	Temperature (°C)	Flow Rate (kg/h)	Pressure (bar)	Composition (mol fraction)
LNG	-162	40.000	1	C ₁ =0,88; C ₂ =0,04; C ₄ =0,015; i-C ₄ =0,02; N ₂ =0,03
Helium	70	75.000	150	He=1
Demin water	25	60.000	1	H ₂ O=1
Boiler Feed water	25	69.692	1	H ₂ O=1

Table 3. Reactor Inlet and Outlet Conditions

Flow	Temperature (°C)	Flow Rate (kg/h)	Pressure (bar)	Composition (mol fraction)
Inlet	23,6339	175.000	1	C ₁ =0,0772; C ₂ =0,0035; C ₃ =0,0013; C ₄ =0,0013; i-C ₄ =0,0017; N ₂ =0,0026; He=0,7746; H ₂ O=0,1377
Outlet	100	175.000	1	C ₂ =0,0035; C ₃ =0,0013; C ₄ =0,0013; i-C ₄ =0,0017; N ₂ =0,0026; CH ₃ OH=0,077; He=0,7746; H ₂ =0,0772; H ₂ O=0,0605

The reaction conduct in this production is adapted from (Bi, et al.) with the reaction mechanism as shown in Figure 1 below.

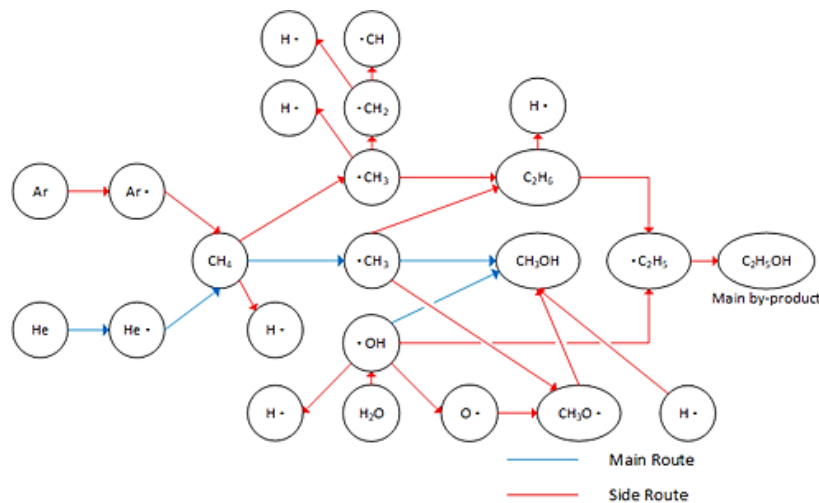


Figure 1. Direct Methane to Methanol Reaction Mechanism

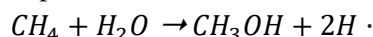
Figure 1 illustrates the direct methane-to-methanol reaction mechanism within a DBD plasma reactor, adapted from prior studies. The figure details the primary (blue) and side (red) pathways involved in transforming methane (CH₄) into methanol (CH₃OH) and other byproducts. In the primary reaction, noble gas helium produces methyl radicals (CH₃·) and hydrogen radicals (H·) when methane interacts with ionized helium plasma (He·). Simultaneously, water molecules dissociate into hydroxyl (OH·) and hydrogen radicals (H·) with the assistance of a TiO₂ catalyst. These methyl radicals react with hydroxyl radicals to form methanol, while byproducts like CH₂, CH radicals, and ethyl radicals (C₂H₅) may lead to ethanol formation. Additionally, a secondary pathway enables methanol formation through reactions between hydrogen and methoxy radicals.

Further research by Bi et al. highlights how argon (Ar) gas can increase electron density in the reactor, enhancing methane activation and the formation of methyl radicals. However, helium (He), which produces higher-energy electrons, achieves greater selectivity and reduces energy requirements. Therefore, this study

utilizes a 2:1 He:CH₄ ratio to maximize methanol selectivity and streamline the separation process by minimizing byproducts.

This investigation's focus on plasma-assisted, single-step methane-to-methanol conversion, underpinned by DBD technology and modeled in DWSim, provides a pathway for industrial-scale applications that could mitigate environmental impacts and improve energy efficiency in methanol production.

This leads us to the primary reaction outlined below, which occurs in both the plasma and liquid phases, resulting in plasma being produced at the plasma interface once the reaction is complete.



2.2 Process and Plant Overview

The methanol production process consists of three key stages: raw material preparation, methanol synthesis, and product purification. Initially, raw materials—including methane sourced from liquefied natural gas (LNG) and high-purity water—undergo preparatory steps to reach optimal conditions for reaction. Methanol synthesis occurs in a Dielectric Barrier Discharge (DBD) reactor, where helium is utilized as an inert gas to enhance reaction efficiency. The final stage involves product purification, where a series of separation and distillation steps ensure the methanol meets the AA-grade quality standard, as depicted in Figure 2, the process flow diagram for this design.

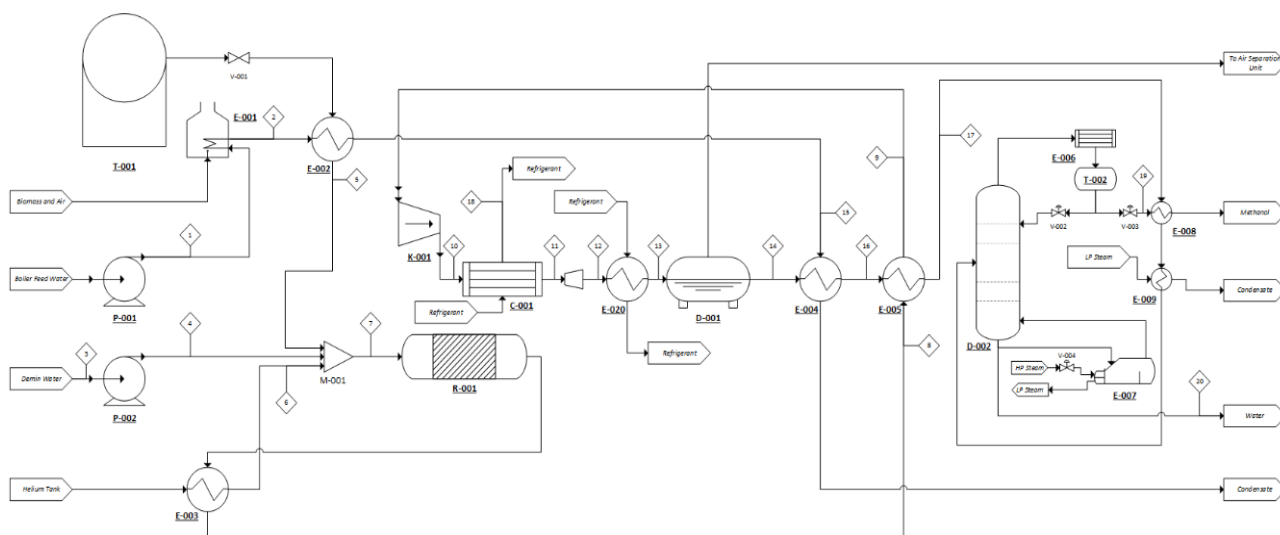


Figure 2. Direct Methane to Methanol Process Flow Diagram

2.2.1 Raw Material Preparation Stage

In the raw material preparation stage, LNG with a methane purity of at least 95% is the primary feedstock. Initially stored at -162°C and 1 bar, the LNG is heated to 300°C and pressurized to 6 bar using high-pressure steam. Helium is introduced at double the molar flow rate of methane, acting as an inert gas to achieve a higher selectivity, as stated by Bi et al. (2019). Water, another essential input, is provided in a high-purity form obtained through seawater desalination using seawater reverse osmosis (SWRO).

2.2.2 Methanol Formation Reaction Stage

Methanol synthesis occurs in the DBD reactor through a plasma-assisted reaction between methane and water. Helium is introduced to generate plasma when an electric current is applied across the reactor's electrodes. This plasma excites helium atoms, facilitating their interaction with methane and water, which enhances methanol production at lower temperatures and atmospheric pressure compared to conventional thermal methods. Plasma technology not only improves reaction efficiency but also reduces emissions. Bi et al. (2019) demonstrated that a helium-to-methane ratio of 2:1 provides optimal selectivity, which would

otherwise decrease sharply in the absence of plasma or helium. Operating conditions are set at 27°C and 1 bar, with a residence time of 1-2 hours to maximize conversion.

2.2.3 Separation Stage

Following synthesis, the gas mixture is cooled to condense methanol, which is then separated from helium using a horizontal separator (D-001). The separated helium is recycled back to the reactor for reuse, while the condensed methanol undergoes further purification. A distillation column (D-002) purifies methanol to a final concentration of 99.85%, meeting AA-grade standards. Before distillation, heat exchangers (E-003, E-005) cool the methanol to facilitate condensation, after which the product is reheated and fed into D-002 for final purification.

2.3 Process Modelling and Simulation

The methanol production plant's mass and energy balances were modeled using DWSim, an open-source chemical process simulator recognized for its application across various fields, including hydrogen production, refrigeration system optimization, and oil and gas plant modeling (Subramanian, 2023; Chantasiriwan, 2023; Andreasen, 2022). DWSim's versatility and wide-ranging applicability made it an ideal choice for this study.

In the simulation, critical parameters such as mass flow rates, temperatures, pressures, and energy consumption were integrated, along with assumptions on LNG purity and plasma efficiency to realistically replicate the production process. This modeling effort provided insights into both the technical feasibility and environmental impact of the plant's operation.

The recent focus on direct methane-to-methanol conversion has underscored the importance of selectivity and efficiency in such processes. Zakaria (2016) reviewed various conversion methods, while Nandy (2022) studied catalysts that support high-selectivity methane oxidation. Li (2023) identified selectivity challenges at high temperatures, which often result in methanol transforming into other derivatives. In response, this study employs a low-temperature plasma reactor to optimize selectivity and maintain methanol as the primary product.

LNG with a minimum methane purity of 95% is used as the primary material, initially at -162°C and 1 bar. It's heated to 300°C and 6 bar using high-pressure steam. Helium, introduced at double the methane molar flow rate. Followed by high-purity water is supplied via seawater desalination through SWRO.

2.4 Economic Analysis

Evaluating the economic feasibility of the low-emission methanol production plant is critical to understanding its potential profitability. Key financial metrics, such as Net Present Value (NPV), Internal Rate of Return (IRR), Payback Period (PBP), and Return on Investment (ROI), were calculated to assess the plant's financial performance.

The plant's total capital expenditure (CAPEX) is estimated at \$479.68 million, with annual operating expenses (OPEX) projected at \$343.65 million, as outlined in Table 5. These CAPEX and OPEX estimates were calculated using multiplication factors based on Garret (2013). With projected annual revenue of \$70.64 million, the plant's net present value (NPV) is calculated at \$171.67 million, and the internal rate of return (IRR) stands at 15.38%, resulting in a payback period of approximately 6.79 years. These financial indicators suggest that, although the plant offers a reasonable return on investment, its profitability remains highly sensitive to fluctuations in methanol prices and carbon credit values.

Table 4. Total Capital Expenditure

Component	Cost (US\$)
Equipment	61,929,557
Site Development	146,153,756
Land and Building	24,771,823
Other	23,285,514
Start-Up	13,971,308
Working Capital	34,928,270
Contractor and Contingency	174,641,352
Total Capital	479,681,580

Table 5. Total Operational Expenditure Calculation without Equity and Depreciation

Component	Cost/year (US\$)
Raw materials, additives, catalysts	199,000,042
Power generation utility	4,644,689
Operational labor and labor-related costs	28,357
Capital related costs	57,817,930
Sales related costs	82,160,517
Total Operational Per Year	343,651,536

We calculated key financial metrics, including Net Present Value (NPV), Internal Rate of Return (IRR), Payback Period (PBP), and Return on Investment (ROI). NPV indicates the value of the project and is used in capital budgeting and investment planning to assess the profitability of the projected investment (Lin and Nagalingam, 2000). Meanwhile, IRR is used to demonstrate the attractiveness of a project and estimate its potential for generating profits. ROI is used to measure the efficiency or profitability of an investment. The Payback Period shows the time required for an investment to return an amount equivalent to the initial investment (Park, 2007). The economic analysis calculations are based on the formulas listed in equations (1), (2), and (3).

$$NPV = \sum_{n=1}^{n=T} \frac{CF_n}{1+i^n} - TCI \quad (1)$$

$$PB = FC + \frac{I}{P+D} \quad (2)$$

$$ROI = \frac{C}{TCI} * 100\% \quad (3)$$

Where CF_n represents the net cash flow during period T, while TCI refers to the total capital investment. The discount rate is denoted by i , and T indicates the number of time periods. FC refers to the depreciable fixed capital investment, i stands for the interest on TCI over the projected service life, P represents the average annual profit, D denotes the average annual depreciation, and C is the annual net profit after taxes. The economic analysis was conducted using Microsoft Excel.

The results of the economic and profitability analysis will provide a comprehensive understanding of the potential economic benefits and risks associated with the operation of this plant. To achieve this, several parameters were considered as follows:

1. The plant will be constructed at the beginning of 2024 and will begin operations in early 2025.
2. Low-emission methanol production will commence in early 2026, with a lifespan of 15 years.
3. Some equipment will have salvage value at the end of its service life.
4. A tax rate of 22% (PwC, 2023).

5. Depreciation is 10% for major equipment and 3% for support equipment and buildings, using the straight-line method (Ministry of Finance, 2023).

Total capital investment encompasses both fixed and working capital, covering all process equipment and auxiliary components. Fixed capital is categorized into direct costs, which are directly related to production, and indirect costs, which are not easily linked to a specific production activity. Working capital accounts for costs such as initial production expenses and inventory costs for raw materials and other supplies. These cost estimations are derived from the indexed time of plant establishment, using the bare module factor as outlined by Seider et al. (2004).

3. RESULT AND DISCUSSION

3.1 Plant Performance and Environmental Analysis

The simulation results from DWSim V8.7.1 were analyzed and scaled up to an industrial level, as illustrated in the process flow diagram (Figure 3). The methanol production process encompasses LNG preheating, reaction, separation, and purification stages. Initially, LNG is preheated from -162°C to 80°C , while water is maintained at 25°C . Helium, used as an inert gas, is then introduced before the mixture enters the reactor at 27°C . The reaction proceeds at a pressure of 1 bar and a temperature of 27°C , with 66 MW/day of electrical energy used to convert methane into methanol via helium plasma. The plasma provides energy that significantly enhances the reaction selectivity, achieving a conversion selectivity of 93% by facilitating efficient methane-to-methanol conversion at lower temperatures. Steam, generated from the combustion of palm shell biomass, provides 6.015 MW/day of the required process energy.

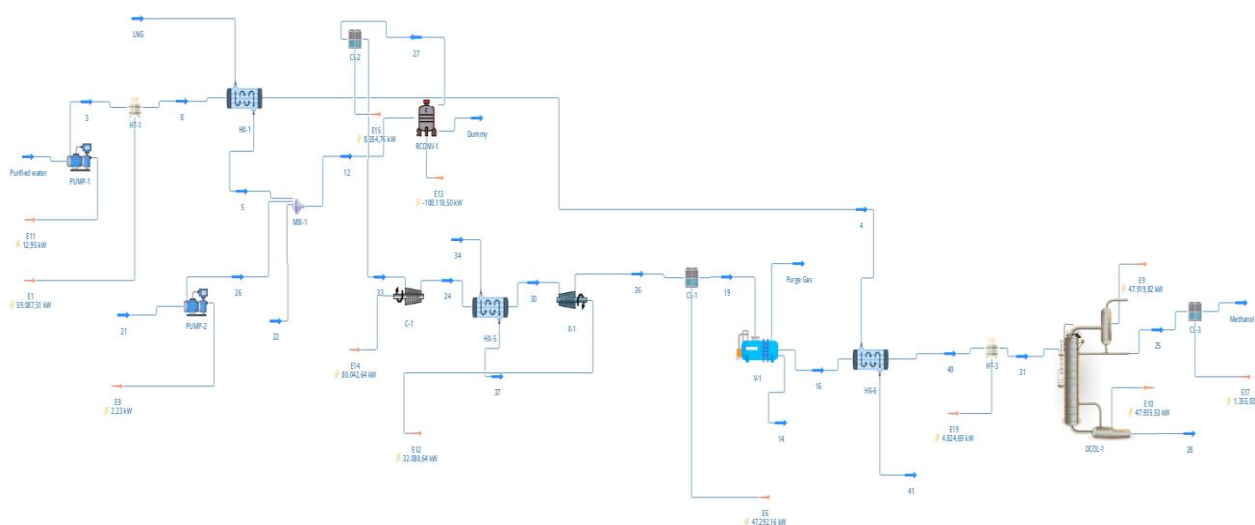


Figure 3. DWSim Simulation Process Flow Diagram

Environmental considerations are integral to the plant design, which emphasizes reduced emissions throughout LNG-based methanol production. During the upstream stage (extraction and processing), CO_2 and CH_4 emissions occur, particularly in regions with lenient flaring and venting regulations. Midstream processes (liquefaction and transport) are energy-intensive, generating CO_2 emissions and potentially releasing CH_4 through leaks in infrastructure. In the downstream stage (regasification and combustion), CO_2 emissions dominate, although CH_4 leaks may persist due to inadequate maintenance.

To address these environmental challenges, renewable energy sources are used to power the plasma generation system, significantly reducing the plant's carbon footprint. Additionally, a carbon capture system utilizing diethanolamine (DEA) captures up to 99.9% of CO_2 emissions, which are subsequently repurposed for secondary processes. This method not only supports the production of blue methanol but also aligns with

sustainable industrial practices by minimizing greenhouse gas emissions. Key performance indicators demonstrate that the integration of renewable energy and carbon capture technologies substantially enhances the environmental performance of the process.

However, economic analysis indicates that the financial viability of low-emission methanol production is sensitive to methanol market prices and carbon credit policies. For the plant to remain competitive with traditional methods, methanol prices must reach \$970 per ton. The introduction of carbon credits could improve economic outcomes, particularly as stricter CO₂ emission penalties are expected in the future.

3.2 Comparative Analysis

While Bi (2019) achieves a conversion selectivity of 93%, recent studies conducted by Huan (2024) report a significantly lower selectivity of 51%, highlighting the variability in performance across different studies. Comparatively, the industrial application of dielectric barrier discharge (DBD) reactors for chemical production remains underexplored, underscoring challenges in demonstrating the economic feasibility of such systems. Although this innovative approach shows potential advantages, such as the possibility of substituting helium with more accessible inert gases or enhancing recycling mechanisms to reduce operational costs, technologies like DBD reactors face significant economic hurdles. For instance, methane-to-methanol conversion using DBD reactors suffers from high energy consumption, extended payback periods, and lower internal rates of return (IRR) compared to conventional methods (Rahimpour et al., 2014; Rahimi et al., 2020). Further optimization is required to improve yields and reduce costs, making these systems less competitive overall.

3.3 Industrial Scalability and Challenges

Scaling this technology to industrial levels involves addressing several challenges, including resource limitations and infrastructure requirements. Helium dependency represents a critical barrier due to its limited global availability and high cost, which is exacerbated by the need for specialized storage and processing infrastructure. These challenges are particularly pronounced in regions like Indonesia, where helium resources and processing capabilities are limited.

Additionally, regulatory frameworks governing carbon credits and emissions play a pivotal role in determining project feasibility. Although current carbon credit prices in Indonesia are relatively low, stricter environmental policies and higher carbon penalty thresholds could improve the economic competitiveness of low-emission methanol production. Moreover, logistical challenges related to LNG handling and biomass combustion require strategic planning to ensure reliable and cost-effective operations.

Despite these obstacles, the plant's reliance on renewable energy sources and its robust carbon capture system positions it as a sustainable alternative to traditional methanol production. However, further studies are needed to evaluate long-term economic impacts, including equipment degradation and fluctuating carbon credit prices, to enhance scalability and cost-effectiveness.

3.4 Economic and Sensitivity Analysis

The economic analysis was calculated using a spreadsheet. The prices of equipment, piping, instrumentation, and buildings were estimated using sizing and price factors from Turton et al. (Turton, 2018). The plant's operating costs were assumed to be a percentage of the investment cost based on Park et al. (Park, 2007). Meanwhile, profitability analyses such as NPV, IRR, PB, and ROI used the equations explained in the previous section for 15 years. A summary of the plant's economic calculation results and profitability analysis is presented in Table 6.

Table 6. Economic Analysis of Low Methanol Emissions from Natural Gas

CAPEX (US\$)	479,681,580
--------------	-------------

OPEX (US\$/year)	343,651,536
Revenue US\$/year)	70,635,332
NPV (US\$)	171,679,332
IRR	15.38%
PBP (years)	6.79
ROI	13.13%

*All financial data are presented in U.S. Dollars (USD) for consistency. Original calculations were conducted in Indonesian Rupiah (IDR) and converted at an exchange rate of IDR 15,774 per USD, effective as of November 7, 2024.

The economic analysis of the proposed methanol production project shows strong profitability, with an ROI of 13.13%, an IRR of 15.38%, and an NPV of \$171.68 million, exceeding the initial investment. The payback period is just 6.79 years, making the project financially attractive (Brockway et al., 2019).

Other studies also support the feasibility of natural gas-based methanol production. For example, one study using an adiabatic pre-reformer reactor model in Aspen HYSYS V10 reported an IRR of 11.73% and an NPV of \$166.63 million (Aletheia & Meyland, 2024). Another study on hybrid steam reforming of glycerol and natural gas confirmed its economic viability (Balegedde Ramachandran et al., 2013).

The economic viability of producing low-emission methanol from LNG is promising but highly dependent on market conditions. As shown in the sensitivity analysis, achieving profitability comparable to conventional methods requires a methanol price of at least \$970 per ton to offset the higher operational costs of low-emission technologies.



Figure 4. Methanol Price per Ton over IRR

Carbon credit pricing is also a critical factor in determining financial performance. While current carbon credit market incentives remain limited, the profitability of low-emission methanol production improves as carbon credit prices rise. For example, at a carbon credit price of \$160/tCO₂, low-emission methanol becomes competitive with gray methanol. However, a carbon price of \$1,200/tCO₂ is required for low-emission methanol to surpass blue methanol in terms of profitability. Sensitivity analyses on CO₂ emission penalties highlight the importance of aligning economic incentives with environmental objectives to sustain long-term profitability.

3.4.1 Levelized Cost of Methanol (LCOM)

The levelized cost of methanol (LCOM) represents the selling price of methanol required to achieve attractive profits relative to its production costs, as formulated by Martin et al (2024).

Table 7 below compares methanol production across three different schemes: gray, blue, and low-emission methanol. Gray methanol, as outlined by IRENA (2021), generates CO₂ emissions without any further treatment. In contrast, blue methanol captures and processes 90% of CO₂ emissions through a carbon capture,

utilization, and storage (CCUS) system. Finally, the production of low-emission methanol focuses on minimizing emissions through improved processes.

Table 7. CO₂ emissions from various types of process

	<i>Gray Methanol</i>	<i>Blue Methanol</i>	This Study
Total CO ₂ emissions from methanol production (tCO _{2e} /tMeOH)	3,10	0,31 (90% captured)	0
LCOM (\$/MeOH)	490	598,81	970

To understand the cost and feasibility of producing methanol sustainably, it's essential to compare three key types: gray, blue, and green methanol. Gray methanol, produced using conventional fossil fuels, has the highest carbon footprint but remains the most cost-effective option. Blue methanol incorporates carbon capture, utilization, and storage (CCUS) technologies, which reduce emissions by capturing CO₂ from production processes, potentially allowing blue methanol to be produced at a levelized cost of approximately \$598 per metric ton. Green methanol, derived from renewable sources like biomass or through the electrolysis of water powered by renewable energy, is the least polluting but also the most costly, with a production cost target of around \$970 per metric ton to achieve comparable profitability to gray methanol.

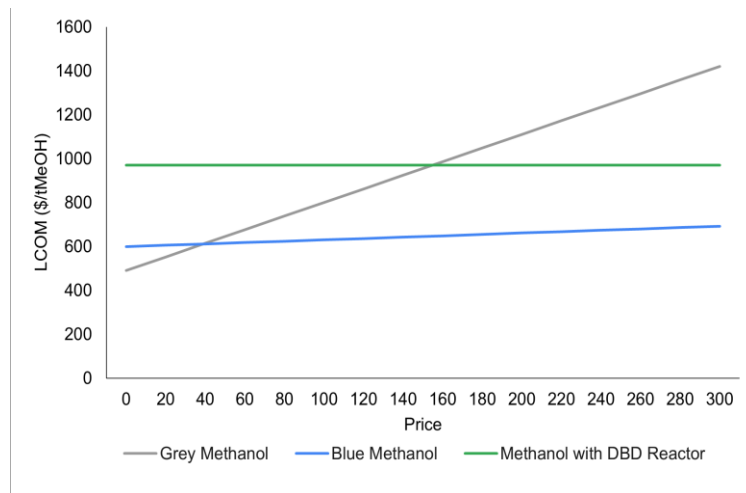


Figure 5. Effect of Levelized Cost of Methanol on Carbon Taxes

Figure 5 illustrates the effect of varying carbon credit prices on methanol profitability, showing that when carbon credits reach \$39 per ton of CO₂, blue methanol becomes more profitable than gray methanol. Green methanol would require a higher credit price of \$160 per ton of CO₂ to surpass gray methanol, and an exceptional credit value of \$1200 per ton of CO₂ to outcompete blue methanol.

The profitability challenge of green methanol is compounded by its higher production costs. By integrating carbon credit incentives, however, the financial gap can be narrowed. With current carbon credits valued at roughly \$4.5 per ton of CO₂ in Indonesia (Indonesia Opens Carbon Trading Market to Both Skepticism and Hope, 2023), the carbon market could play a pivotal role in enhancing the competitiveness of low-emission methanol.

Thus, while green methanol holds potential for future profitability in a stricter regulatory environment, current carbon credit levels make it economically challenging to exceed blue methanol's profitability. This analysis underscores the need for further policy support to make sustainable methanol solutions financially viable in the long term.

3.4.2 Levelized Cost of Electricity (LCOE)

The Levelized Cost of Electricity (LCOE) is a method used to calculate the average cost of electricity generated by an asset over its operational lifetime. This metric is commonly used to compare electricity costs across various energy sources or projects, providing a standardized framework for evaluation. Simply put, LCOE represents the cost per unit of electricity produced over the lifetime of a generating asset (Levelized Cost of Energy (LCOE), 2024).

In the context of the methanol plant, LCOE calculations are essential for evaluating potential cost savings related to both process and non-process energy usage. Given the plant's reliance on energy-intensive equipment such as pumps, compressors, and plasma reactors, determining the LCOE of the electricity supply is critical for assessing the efficiency of the designed power generation system. Based on the analysis, the LCOE for this plant is calculated to be Rp 723,517,318 per megawatt (MW) per year.

4. CONCLUSIONS

This study presents the design of a methanol production plant with a capacity of 500,000 tons per year, utilizing natural gas as the primary feedstock. The process involves natural gas purification, a direct methane-to-methanol conversion using a Dielectric Barrier Discharge (DBD) reactor, and subsequent methanol separation and purification. The simulation results confirm that the process can produce methanol with AA-grade purity while significantly reducing carbon emissions.

From an economic perspective, the plant demonstrates profitability with an IRR of 15.38% and a payback period of 6.79 years, making it a viable investment under current market conditions. However, profitability remains sensitive to methanol prices and carbon credits, highlighting the need for supportive environmental policies. Overall, this study provides a foundation for sustainable methanol production and contributes to Indonesia's efforts to achieve self-sufficiency in chemical production while reducing environmental impact.

The simulation modeled using DWSim demonstrates that this process can produce methanol with AA grade quality. From an economic perspective, financial analysis indicates that investment in this plant is profitable, with an IRR of 15.38%, a payback period of 6.79 years, and an ROI of 13.13%. Therefore, this plant can be considered a viable project to support government policies related to low-emission plants. Overall, this design provides a foundation for the implementation of a sustainable and economical methanol production plant from natural gas and contributes to efforts to achieve chemical production self-sufficiency and national environmental targets.

5. ACKNOWLEDGMENTS

We would like to express our gratitude to our colleagues at the Calvin Institute of Technology who supported the authors in conducting this research study

6. REFERENCES

- Al-Rowaili, F. N., Khalafalla, S. S., Al-Yami, D. S., Jamal, A., Ahmed, U., Zahid, U., & Al-Mutairi, E. M. (2022). Techno-economic evaluation of methanol production via gasification of vacuum residue and conventional reforming routes. *Chemical Engineering Research and Design*, 177, 365–375. <https://doi.org/10.1016/j.cherd.2021.11.004>
- Aletheia, S. P., & Meyland, M. (2024a). Techno-economic analysis of blue methanol production from natural gas with carbon capture in Indonesia. *International Journal of Engineering Continuity*, 3(2), 54–68. <https://doi.org/10.58291/ijec.v3i2.288>
- Andreasen, A. (2022). *Evaluation of an Open-source Chemical Process Simulator Using a Plant-wide Oil and Gas Separation Plant Flowsheet Model as Basis*. *Periodica Polytechnica Chemical Engineering*, 66(3), 503–511. <https://doi.org/10.3311/ppch.19678>
- Badan Pusat Statistik. (n.d.). Kaltim.bps.go.id. <https://kaltim.bps.go.id/indicator/6/310/1/upah-minimum-regional.html>

- Balegedde Ramachandran, R. P., Oudenhoven, S. R., Kersten, S. R., van Rossum, G., & van der Ham, A. G. (2013). Techno-economic analysis of biomethanol production via hybrid steam reforming of glycerol with natural gas. *Energy & Fuels*, 27(10), 5962–5974. <https://doi.org/10.1021/ef401323w>
- Bi, W., Tang, Y., Li, X., Dai, C., Song, C., Guo, X., & Ma, X. (2022). One-step direct conversion of methane to methanol with water in non-thermal plasma. *Communications Chemistry*, 5(1), 1–6. <https://doi.org/10.1038/s42004-022-00735-y>
- Chantasiriwan, S. (2023). Simulation and Optimization of Vapor Absorption Refrigeration System Using Dwsim. *Chemical Engineering Transactions*, 100, 613-618. <https://doi.org/10.3303/CET23100103>
- ERIA (2021), 'Outlook of LNG Production', in Kimura, S., et al. (eds.), Feasible Solutions to Deliver LNG to Midsized and Large Islands in Indonesia. ERIA Research Project Report FY2020 no.18, Jakarta: ERIA, pp.31-35.
- IEA (International Energy Agency). 2021. *Methanol Production and Its Role in a Clean Energy Transition*. International Energy Agency, Paris.
- IRENA – International Renewable Energy Agency. (2021). www.irena.org. <http://www.irena.org/publications>
- Isaac, J. (2023, December 4). *Indonesia secures climate collaborations at COP28, inking milestone agreements | Lobby - Indonesia Business Post*. Indonesia Business Post. <https://indonesiabusinesspost.com/lobby/indonesia-secures-climate-collaborations-at-cop28-inking-milestone-agreements/>
- Jong, H. N. (2023, October 12). *Indonesia opens carbon trading market to both skepticism and hope*. Mongabay Environmental News. <https://news.mongabay.com/2023/10/indonesia-opens-carbon-trading-market-to-both-skepticism-and-hope/#:~:text=Each%20metric%20ton%20of%20carbon>
- Kourkoumpas, D. S., Papadimou, C. D., Karellas, S., Leontaritis, A. D., Panopoulos, K. D., & Kakaras, E. (2018). A review of methanol production from biomass. *Energies*, 11(5), 1-27. <https://doi.org/10.3390/en11051125>
- Levelized cost of energy (LCOE). Corporate Finance Institute. (2024, January 12). <https://corporatefinanceinstitute.com/resources/valuation/levelized-cost-of-energy-lcoe/>
- Li, S., Ahmed, R., Yi, Y., & Annemie Bogaerts. (2021). Methane to Methanol through Heterogeneous Catalysis and Plasma Catalysis. *Catalysts*, 11(5), 590–590. <https://doi.org/10.3390/catal11050590>
- Li, Z., Chen, Y., Xie, Z., Song, W., Liu, B., & Zhao, Z. (2023). Rational Design of the Catalysts for the Direct Conversion of Methane to Methanol Based on a Descriptor Approach. *Catalysts*, 13(8), 1226. <https://doi.org/10.3390/catal13081226>
- Lin, G. C. I., & Nagalingam, S. V. (2000). *CIM justification and optimisation*. Taylor & Francis.
- Marcel Ginu Popa, Niculae Negurescu, Pana, C., & Alexandru Racovitz. (2001). Results Obtained by Methanol Fuelling Diesel Engine. *SAE Technical Paper Series*. <https://doi.org/10.4271/2001-01-3748>
- Martin, J. A., Tan, E. C. D., Ruddy, D. A., King, J., & To, A. T. (2024). *Temperature–Pressure Swing Process for Reactive Carbon Capture and Conversion to Methanol: Techno-Economic Analysis and Life Cycle Assessment* (NREL Report No. 88329). National Renewable Energy Laboratory.
- Maulana, M. R. (2021, February 5). *Daya Pacu Industri Metanol*. Bisnis.com. <https://ekonomi.bisnis.com/read/20210205/44/1352775/daya-pacu-industri-metanol>
- Menteri Keuangan. (2023). *PERATURAN MENTERI KEUANGAN REPUBLIK INDONESIA NOMOR 72 TAHUN 2023 1–76*. (Original work published 2023)
- Nandy, A., Duan, C., Goffinet, C., & Kulik, H. J. (2022). New Strategies for Direct Methane-to-Methanol Conversion from Active Learning Exploration of 16 Million Catalysts. *JACS Au*, 2(5), 1200–1213. <https://doi.org/10.1021/jacsau.2c00176>
- Parderio, P. T., Dharmawan, A. D., Wibawa, G., & Wiguno, A. (2022). Pra Desain Pabrik Metanol dari Gas Alam. *Jurnal Teknik ITS*, 11(3). <https://doi.org/10.12962/j23373539.v11i3.98722>
- Park, C. S. (2007). *Contemporary engineering economics*. Prentice Hall.

- Pröll, T., & Lyngfelt, A. (2022). Steam Methane Reforming with Chemical-Looping Combustion: Scaling of Fluidized-Bed-Heated Reformer Tubes. *Energy & Fuels*, 36(17). <https://doi.org/10.1021/acs.energyfuels.2c01086>
- PwC. (2023). *Indonesia Pocket Tax Book 2023*. (Original work published 2023)
- R. Turton, J. Shaeiwitz, D. Bhattacharyya, W. Whiting, Analysis, Synthesis, and Design of Chemical Processes, 5 ed. Pearson Publishing, 2018.
- Román-Leshkov, Y., & Dumesic, J. A. (2014). Catalysis for renewable fuel production from biomass-derived carbohydrates. *Nature Chemistry*, 6(10), 801-813. <https://doi.org/10.1038/nchem.2042>
- Seider, W., Seader, J., Lewin, D., 2004. Product and process design principles: synthesis, analysis, and evaluation.
- Subramanian, G., & Neelameggham, N. R. (2023). Process Simulation for Low Emission Hydrogen Production Using DWSIM. *the Minerals, Metals & Materials Series*, 1144-1154. https://doi.org/10.1007/978-3-031-22524-6_107
- Suseno, T., & Umar, D. F. (2021). Prospect of coal-based methanol market in Indonesia. *IOP Conference Series: Earth and Environmental Science*, 882(1), 012073. <https://doi.org/10.1088/1755-1315/882/1/012073>
- Yang, S., Liang, B., & Feng, L. (2019). Comparative life cycle assessment of methanol and conventional fuels: Implications for greenhouse gas emissions. *Journal of Cleaner Production*, 206, 172-183. <https://doi.org/10.1016/j.jclepro.2018.09.108>
- Yusuf, N., & Tareq Al-Ansari. (2023). Current and Future Role of Natural Gas Supply Chains in the Transition to a Low-Carbon Hydrogen Economy: A Comprehensive Review on Integrated Natural Gas Supply Chain Optimisation Models. *Energies*, 16(22), 7672-7672. <https://doi.org/10.3390/en16227672>
- Zakaria, Z., & Kamarudin, S. K. (2016). Direct conversion technologies of methane to methanol: An overview. *Renewable and Sustainable Energy Reviews*, 65, 250-261. <https://doi.org/10.1016/j.rser.2016.05.082>
- Zheng, J., Ye, J., Ortuño, M. Á., Fulton, J. L., Gutiérrez, O. Y., Camaioni, D. M., Radha Kishan Motkuri, Li, Z., Webber, T., B. Layla Mehdi, Browning, N. D., R. Lee Penn, Farha, O. K., Hupp, J. T., Truhlar, D. G., Cramer, C. J., & Lercher, J. A. (2019). Selective Methane Oxidation to Methanol on Cu-Oxo Dimers Stabilized by Zirconia Nodes of an NU-1000 Metal-Organic Framework. *Journal of the American Chemical Society*, 141(23), 9292-9304. <https://doi.org/10.1021/jacs.9b02902>

Experimental Laser Cutting Material Removal Rate for Polymethylmethacrylate in Construction Applications

Muhammad Ikhsan¹, Nurhidayanti^{2,*}, Budiawan Sulaeman³

¹ Department Mechanical Engineering, Politeknik Bosowa, Makassar, Indonesia

² Department Mechanical Engineering, Politeknik Negeri Ujung Pandang, Makassar, Indonesia

³ Andi Djemma University, Palopo, Indonesia

* Corresponding Author E-mail: nurhidayantisamsir@poliupg.ac.id

Abstract

This research aims to optimize the laser cutting process on polymethylmethacrylate (PMMA) to improve efficiency and quality in construction applications. By exploring the influence of variations in laser current, cutting speed, and material thickness, this study sought to identify the optimal parameters that resulted in the highest material removal rate (MRR) with minimal overcut. Through a series of experiments testing various parameter combinations, the study found that a cutting speed of 40 mm/s, laser current of 80 A, and material thickness of 3 mm yielded the best cutting performance. The results show that optimization of laser cutting parameters can significantly improve the precision, energy efficiency, and quality of PMMA cutting results. The implications of these findings are significant for the development of more efficient and sustainable laser cutting techniques, supporting the use of PMMA in various innovative construction applications such as facades, decorative elements, and architectural prototypes. This research contributes to the understanding of PMMA laser cutting process optimization, with the potential to expand the application of this material in the construction industry through more efficient and quality fabrication methods.

Keywords:

Construction Application; Laser Cutting; Material Removal Rate; Overcut; Polymethylmethacrylate

1. INTRODUCTION

In the manufacturing and construction industries, laser cutting has emerged as a revolutionary machining process widely applied for precision cutting and material shaping. This method, particularly CO₂ laser cutting, offers advantages such as low cost, fast processing and high-quality results, making it an ideal choice for applications where accuracy and efficiency are required (Zhou & Mahdavian, 2004).

Laser cutting works by melting or vaporising the material to form precision walls along the cutting path, which can be customised for various material depths or thicknesses. The technology supports a wide range of materials, including metals, polymers and composites, enabling versatile applications in construction, such as intricate panel design, structural prototyping and advanced material customisation (Moradi et al., 2021).

Polymethylmethacrylate (PMMA) is a polymer widely used in construction due to its superior physical properties, such as high transparency, light weight, and ease of moulding, making it suitable for decorative facades, light diffusers, and structural components in modern architecture (Monsores et al., 2019). PMMA material is thermal properties, such as its low thermal diffusion (7×10^{-7} m²/s) and melting range around 300°C, contribute to improved cutting quality and reduced processing time during laser machining (Khoshaim et al., 2021). These qualities make PMMA an excellent candidate for sustainable construction materials where precision and efficiency are critical.

Previous research has shown that laser cutting parameters-such as cutting speed, laser power, and material thickness-play an important role in determining material removal rate (MRR), surface quality, and overall efficiency. Sharifi and Akbari (2019) shows that optimal laser power and speed are essential to achieve smooth cutting on metal alloys, a principle that applies equally to polymers such as PMMA. High cutting speeds

doi http://dx.doi.org/10.51557/pt_jiit.v10i1.3074

article history: Received December 09, 2024; Received in revised from March 04, 2025; Accepted March 04, 2025;
Available online March 25, 2025.

This is an open access article under the [CC-BY-SA](https://creativecommons.org/licenses/by-sa/4.0/) license



minimise kerf width, while precise power and speed control ensure heat affected zone (HAZ) reduction and improved edge quality (Moradi et al., 2021). Furthermore, Moghadasi et al. (2021) PMMA exhibits superior performance in reducing kerf width and HAZ compared to other polymers such as polycarbonate (PC) and polypropylene (PP), making it ideal for construction projects requiring high precision.

However, while previous research has explored the influence of laser cutting parameters on various materials, there are significant gaps in the understanding of CO₂ laser cutting parameter optimisation specific to PMMA in the context of construction applications. In particular, the influence of the combination of cutting speed, laser current and material thickness on MRR and overcut on PMMA, as well as the implications for yield quality and energy efficiency, is less explored in depth. This research aims to fill this gap by systematically investigating the influence of these parameters, with a focus on optimisation for sustainable and innovative construction applications. The results of this research are expected to contribute to the development of more efficient and high-quality laser-cutting techniques and expand the application of PMMA in construction elements such as facades, decorative structures and architectural prototypes.

Laser cutting technology is invaluable in construction to produce complex geometries such as curved panels, decorative facades and modular structural components. Recent advances in CO₂ laser cutting enable efficient material processing while maintaining a high-quality finish, reducing production time and costs. This paper focuses on optimising the laser cutting parameters of PMMA polymers-cutting speed, laser current and material thickness-to increase the material take-up rate and minimise overcut. By addressing these factors, this research aims to support the development of sustainable, efficient and high-precision manufacturing techniques customised for construction applications.

2. METHODS

Polymethylmethacrylate is the material used in this work, a generally applicable material. Figure 1 shows an illustration the laser cutting process on PMMA materials with thicknesses of 3 mm and 5 mm. The process begins with machine control via a computer, which configures parameters such as laser power, gas pressure, and cutting speed. A lens focuses the laser beam to concentrate energy at a specific point on the material's surface, enabling precise cuts. An assist gas, such as nitrogen or oxygen, is directed through a nozzle to clear molten material from the cutting area, ensuring smooth and defect-free cuts. The resulting cut path (kerf) is assessed based on the quality of the top and bottom surfaces, the cut width, and the heat-affected zone (HAZ) to verify the effectiveness of the chosen cutting parameters.

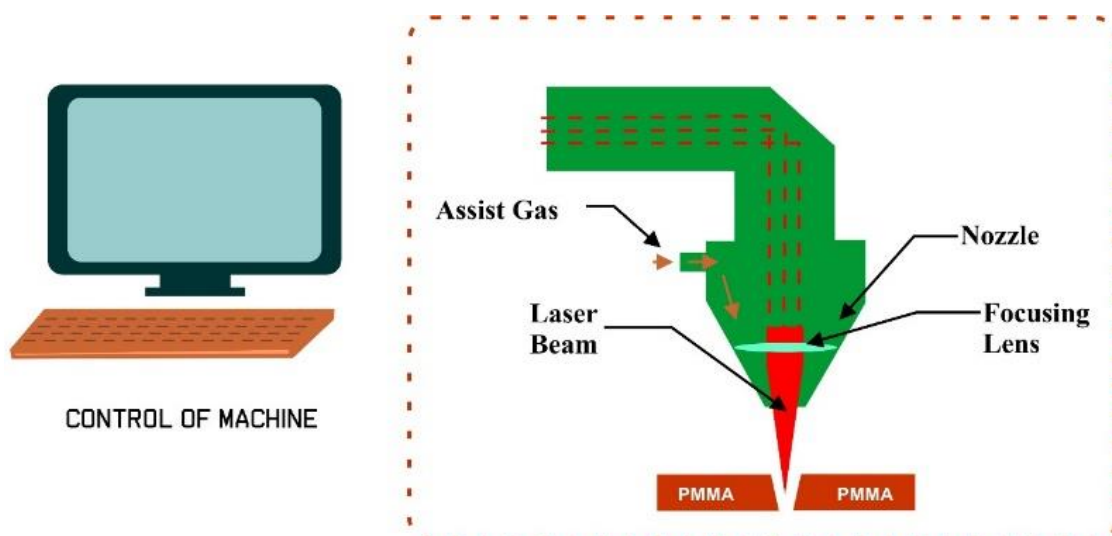


Figure 1. Illustration of laser cutting used PMMA

The parameters used in this work are shown in Table 1. while the PMMA cutting illustration, showing the difference in size at the top and bottom as well as the material thickness, can be seen in Figure 2.

Table 1. Parameters used in research

No	Parameter Process	Units	Process Parameter Value		
			Low	Medium	High
1	Laser cutting	Ampere (A)	60	70	80
2	Cutting speed	mm/s	20	30	40
3	Thickness	mm	3	-	5

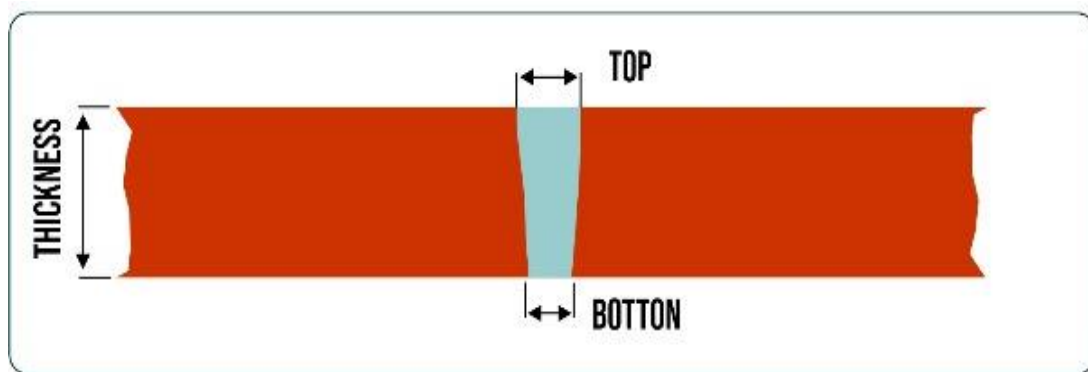


Figure 2. Illustration of PMMA cutting profile of 3 mm and 5 mm thickness

Table 2. Properties of PMMA (Khoshaim et al., 2021)

No	Properties	Values
1	Density	1188 kg/m ³
2	Thermal conductivity	0.193 W.m ⁻¹ K ⁻¹
3	Heat capacity	1.42 kJ kg ⁻¹ K ⁻¹
4	Flammability UL94	HB
5	Thermal expansion coefficient	7 x 10 ⁻⁵ K ⁻¹
6	Thermal diffusivity	7 x 10 ⁻⁷ m ² /s
7	Melting temperature	433 K
8	Water absorption	0.3 %
9	Ultimate strength	72.4 MPa

3. RESULT AND DISCUSSION

This section presents the research results and analyses obtained based on the specified parameters. The discussion focuses on the interpretation of data from the PMMA cutting process, by analysing the influence of variables on the Material Removal Rate (MRR) and overcut produced.

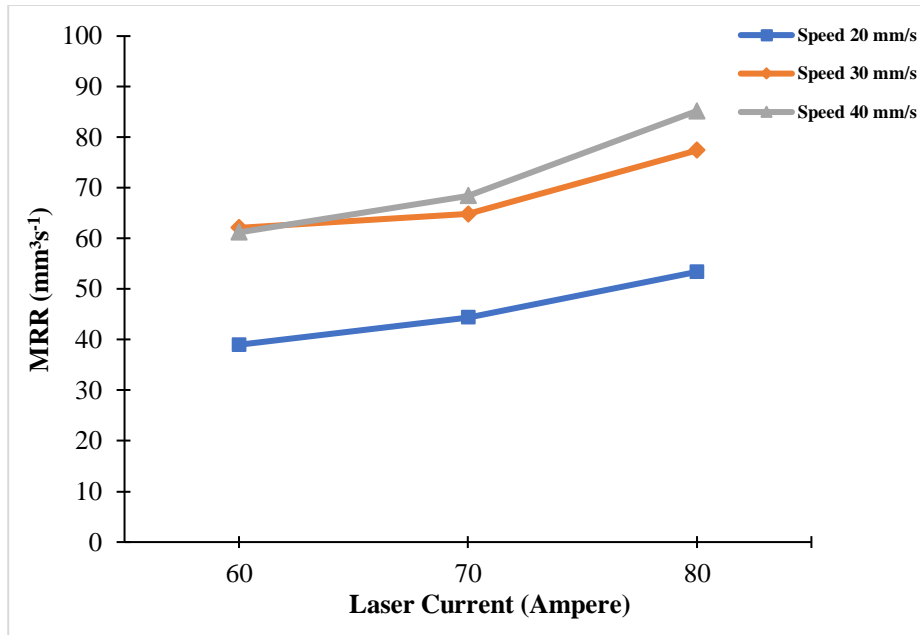


Figure 3. The result Material Removal Rate (MRR) of thickness 3 mm

The graph illustrates the relationship between laser current and Material Removal Rate (MRR) at varying nozzle speeds of 20 mm/s, 30 mm/s, and 40 mm/s. Figure 3 presents a linear trend, indicating that the MRR value rises proportionally with an increase in laser current and nozzle speed during the laser cutting process. Based on the results obtained, it can be seen in Figure 3. the movement of the nozzle displacement with a speed of 20 mm/s obtained an MRR value of $39 \text{ mm}^3\text{s}^{-1}$ with a laser current of 60 A. While the maximum value is obtained from the use of a speed of 40 mm/s with an MRR value of $86 \text{ mm}^3\text{s}^{-1}$ with a laser current of 80 A. It can be assumed that higher nozzle speeds also produce greater MRR at large laser current levels, resulting in the efficiency of laser energy distribution in removing material. This finding is in line with a study by Choudhury and Shirley (2010) which confirmed that a significant increase in laser power and travelling speed would increase MRR without affecting the quality of the cut if the parameters are within optimal limits. A high increase in MRR indicates the successful efficiency of the manufacturing process. However, it is likely to affect decreasing surface quality if the parameter selection is not set appropriately (Wang et al., 2021).

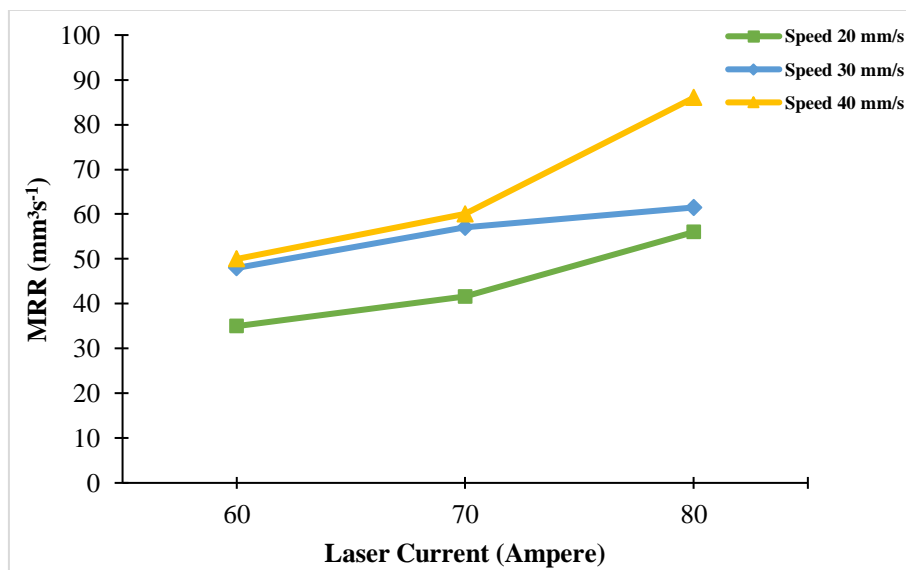


Figure 4. The result Material Removal Rate (MRR) of thickness 5 mm

Based on the graph shown in Figure 4, increasing the Laser Current from 60 A to 80 A provides a consistent increase in the MRR at cutting speeds. This indicates that the thermal energy generated by the laser increases with high current, accelerating the ablation process of PMMA material more efficiently. High cutting speed (40 mm/s) with 80 A current achieved the highest MRR. This is because the laser interaction time with the material is short enough that the energy generated is focused on material removal, without causing heat accumulation that can reduce efficiency. Meanwhile, at low speed (20 mm/s) with a current of 60 A, it is only $35 \text{ mm}^3\text{s}^{-1}$, where longer laser exposure causes melting of excess material that accumulates on the surface, thus inhibiting maximum material removal (Kumar & Babu, 2024). It should be noted based on the low laser current parameter graph that the energy generated is not large enough to optimally support high speeds. As a result, the MRR between speeds (20 mm/s, 30 mm/s, and 40 mm/s) shows an insignificant difference. However, at low laser current, as shown in the graph, 80 A, the MRR increases, especially at high speed, indicating that the combination of high current and high speed is an efficient relationship with PMMA thickness around 5 mm.

Based on the MRR results with graphical comparison Figure 3. is the MRR result with a PMMA cutting thickness of 3 mm while Figure 4 shows at a cutting thickness of 5 mm, there is a significant difference from the resulting MRR value which has decreased. The MRR value obtained tends to decrease as the material thickness increases (Hashemzadeh & Pourshaban, 2020). This is due to the process of material removal in PMMA due to the absorption of laser energy which causes the material to evaporate and melt quickly so that the level of cutting efficiency is affected by the laser energy absorbed by the material.

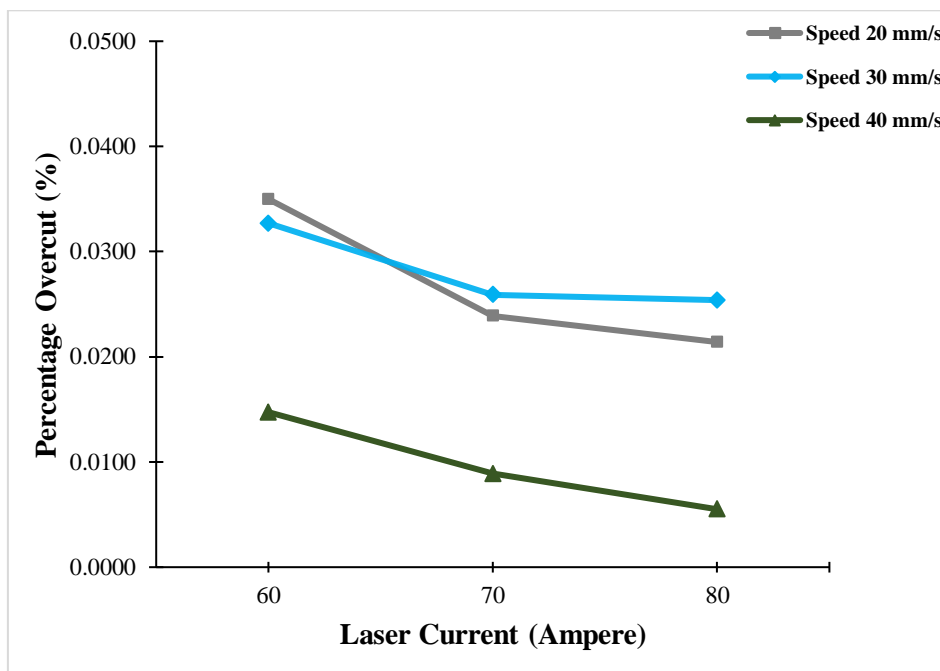


Figure 5. The result Overcut of thickness 3 mm

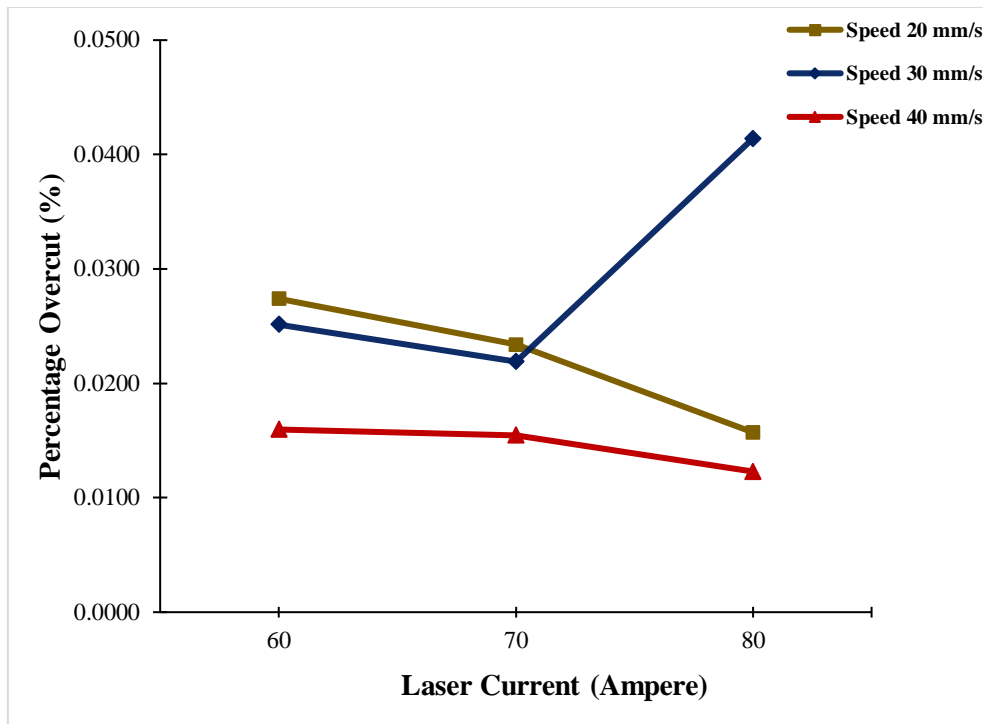


Figure 6. The result Overcut of thickness 5 mm

The cutting speed significantly affects the occurrence of the overcut phenomenon in the process. Based on the data shown in the graph, increasing the cutting speed significantly reduces the overcut value. At low speeds, such as 20 mm/s, the overcut reaches 0.0350% at a current of 60 A, while at a high speed of 40 mm/s, the overcut value decreases drastically to 0.0055%. This occurs because low speeds provide longer laser exposure times, causing excessive melting around the cut area, while high speeds limit such melting. In addition, increasing the laser current from 60 A to 80 A also resulted in a decrease in overcut as the greater thermal energy helped to remove material in a more efficient and focused manner. The material thickness affects the overcut results, where PMMA a thickness of 5 mm produces a lower overcut than PMMA with a thickness of 3 mm. This is because the thermal energy distribution in thicker material does not reach the bottom kerf area, so the material is not completely cut and results in a smaller overcut. In contrast, thinner materials have more significant melt due to wider energy distribution.

The findings of a study conducted by Yusuf (2024) confirmed that higher amperage can improve the precision of the cut, which can reduce the occurrence of overcut. Therefore, based on the findings of this study, the optimal parameter combination—high cutting speed (40 mm/s) and high laser current (80 A) was found to be effective in reducing overcut and improving the efficiency of the laser cutting process, particularly for PMMA.

4. CONCLUSIONS

This study shows that the optimal laser cutting parameters for Polymethylmethacrylate (PMMA), such as a cutting speed of 40 mm/s, a laser current of 80 Ampere, and a material thickness of 3 mm, resulted in an excellent Material Removal Rate (MRR) of 86 mm³/s, with a minimum overcut of 0.0055%. These parameters not only improve material removal efficiency but also ensure precise cutting, which is critical for construction applications requiring high-quality PMMA components. This study highlights the importance of controlling the laser speed and current to reduce excessive melting and maintain a clean, high-precision cut, making these

findings highly relevant to manufacturing in the construction industry where precision and material integrity are important.

5. ACKNOWLEDGMENTS

Thank you very much to the Department of Mechanical Engineering, State Polytechnic of Ujung Pandang and Bosowa Polytechnic Laboratory, Makassar for contributing and supporting the publication of this research article.

REFERENCES

- Choudhury, I. A., & Shirley, S. (2010). Laser cutting of polymeric materials: An experimental investigation. *Optics and Laser Technology*, 42(3), 503–508. <https://doi.org/10.1016/j.optlastec.2009.09.006>
- Hashemzadeh, M., & Pourshaban, R. (2020). The Effect of Power, Maximum Cutting Speed and Specific Point Energy on the Material Removal Rate and Cutting Volume Efficiency in CO2 Laser Cutting of Polyamide Sheets. *Journal of Modern Processes in Manufacturing and Production*, 9(3).
- Khoshaim, A. B., Elsheikh, A. H., Moustafa, E. B., Basha, M., & Showaib, E. A. (2021). Experimental investigation on laser cutting of PMMA sheets: Effects of process factors on kerf characteristics. *Journal of Materials Research and Technology*, 11, 235–246. <https://doi.org/10.1016/j.jmrt.2021.01.012>
- Kumar, K. N., & Babu, P. D. (2024). Investigation on Polymer Hybrid Composite Through CO2 Laser Machining for Precise Machining Conditions. *International Journal of Precision Engineering and Manufacturing*, 25(5), 1043–1061. <https://doi.org/10.1007/S12541-023-00942-0/METRICS>
- Moghadasi, K., Tamrin, K. F., Sheikh, N. A., & Jawaid, M. (2021). A numerical failure analysis of laser micromachining in various thermoplastics. *International Journal of Advanced Manufacturing Technology*, 117(1–2), 523–538. <https://doi.org/10.1007/S00170-021-07428-1/METRICS>
- Monsores, K. G. D. C., Silva, A. O. Da, De Sant'Ana Oliveira, S., Rodrigues, J. G. P., & Weber, R. P. (2019). Influence of ultraviolet radiation on polymethylmethacrylate (PMMA). *Journal of Materials Research and Technology*, 8(5), 3713–3718. <https://doi.org/10.1016/j.jmrt.2019.06.023>
- Moradi, M., Moghadam, M. K., Shamsborhan, M., Beiranvand, Z. M., Rasouli, A., Vahdati, M., Bakhtiari, A., & Bodaghi, M. (2021). Simulation, statistical modeling, and optimization of CO2 laser cutting process of polycarbonate sheets. *Optik*, 225. <https://doi.org/10.1016/j.ijleo.2020.164932>
- Sharifi, M., & Akbari, M. (2019). Experimental investigation of the effect of process parameters on cutting region temperature and cutting edge quality in laser cutting of AL6061T6 alloy. *Optik*, 184, 457–463. <https://doi.org/10.1016/j.ijleo.2019.04.105>
- Wang, B., Liu, Z., Cai, Y., Luo, X., Ma, H., Song, Q., & Xiong, Z. (2021). Advancements in material removal mechanism and surface integrity of high speed metal cutting: A review 2 mechanism; Surface integrity; Cutting force and temperature; Cutting tools. *International Journal of Machine Tools and Manufacture*, 166(103744).
- Yusuf, A. (2024). THE EFFECT OF CUTTING SPEED ON CUTTING QUALITY WITH LASER CUTTING MACHINE. *REVIEW OF MULTIDISCIPLINARY EDUCATION*, 3(4). <https://ojs.transpublika.com/index.php/ROMEO/>
- Zhou, B. H., & Mahdavian, S. M. (2004). Experimental and theoretical analyses of cutting nonmetallic materials by low power CO2-laser. *Journal of Materials Processing Technology*, 146(2), 188–192. <https://doi.org/10.1016/j.jmatprotec.2003.10.017>

Sustainability Strategy for Makassar City Central Waste Bank

Azizah Putri Abdi^{1, *}, Rasdiana¹, Yan Radhinal¹, Tri Wahyuningsih¹, Andi Idham Asman¹

¹ Urban and Regional Planning Study Program, Faculty of Engineering, Universitas Tadulako, Palu City, Indonesia

* Corresponding Author E-mail: azizahputriabdi@untad.ac.id

Abstract

Waste banks solve the waste problem by involving the community in waste sorting and processing, which contributes to improving the local economy. This research aims to explore the implementation of the performance of waste banks from economic, social, and environmental aspects, as well as the sustainability strategy of waste banks in Makassar City. This research uses qualitative descriptive analysis. The results showed that waste banks in Makassar City have fulfilled two pillars of sustainability: economic and environmental. This is evident from the increased income of the community, especially the low-income ones, and the effectiveness of waste management that supports waste reduction. However, these waste banks still face social challenges, mainly related to the community's low participation and the manager's non-optimal role. To improve sustainability, this study proposes several strategies, such as increasing community participation through socialisation and social media to educate the importance of waste management, affirming waste sorting regulations, strengthening the role of waste bank managers, and improving facilities and infrastructure that support waste bank operations. Implementing these strategies is expected to ensure that waste banks in Makassar City operate sustainably.

Keywords:

Makassar City; Sustainability; Waste Management; Waste Bank;

1. INTRODUCTION

Makassar is one of the largest cities in Indonesia. Solid waste is a major problem in this city, where the volume of waste in Makassar City reaches 1,048 tons/day (Dinas Lingkungan Hidup Kota Makassar, 2024). The challenges faced in waste management in Makassar City are the lack of awareness and behaviour of residents, as well as attention from the government (Susan et al., 2023), inadequate infrastructure (Rumata et al., 2025), and the need for a waste sorting approach to reduce the overcapacity of Makassar City Landfill (Rusni, 2024). There is a new paradigm in waste management, as stated in Law Number 18 of 2008, which introduces waste management with two approaches, namely waste reduction and handling through 3R or reduce, reuse, and recycle (Kementerian Lingkungan Hidup dan Kehutanan, 2021). To support these efforts and to overcome the challenges of waste management in Makassar City, the government encourages its citizens to care for, sort, and voluntarily carry their waste by setting up a waste bank, where certain waste is traded for money. This system not only incentivises waste sorting but also involves the community and the local government. The operation of these waste banks hinges on the active participation of the public, which plays a vital role in gathering and sorting waste before it is exchanged at the banks. This communal participation also stimulates local economic activities, as residents earn income from selling waste collected at the banks.

However, despite its positive impact, the waste bank has not alleviated the problem of poverty, but it still has an impact on the community, both for itself and the surrounding environment (Wulandari et al., 2017). The research (Masrurroh et al., 2022), shows that a waste bank can significantly impact the socio-economy of the community. In Banten, it amounts to 41.5%, where the savings from the waste bank can help buy daily necessities. Research by (Fatmawati et al., 2024) also shows that the role of waste banks consistently improves economic outcomes, which is inseparable from community participation, and improves government performance in waste management. Furthermore, the implementation of waste banks itself is related to the concept of a circular economy, where the main objective of this concept is to reduce waste and maximise existing resources (Nur, 2021; Satori et al., 2020). The circular economy promotes sustainable production

doi http://dx.doi.org/10.51557/pt_jiit.v10i1.3156

article history: Received January 14, 2025; Received in revised from March 21, 2025; Accepted March 22, 2025;
Available online March 25, 2025.

This is an open access article under the **CC-BY-SA** license



practices by extending the value of waste into raw materials that can be recycled into new products (Fatmawati et al., 2024).

The concept of sustainable development is deeply integrated into Indonesia's growth policies, focusing on the development aspects (Setyarini et al., 2020). While driving economic progress, population growth also impacts the environment, particularly regarding waste production. Effective waste management is, therefore, essential in achieving sustainable development targets, as it has significant implications for society and the economy (Aminah & Muliawati, 2021). The Sustainable Development Goals (SDGs) most relevant to waste management are Goal 3, which focuses on ensuring healthy living, and Goal 8, which promotes economic growth, full employment, and decent work for all (Saleh et al., 2020; Schroeder et al., 2019). Sustainability indicators can be used to assess waste management performance from economic, environmental, and social perspectives (Khair, 2019; Setyarini et al., 2020).

Considering the increasingly complex waste management problems and their impact on the environment and community welfare, this study is expected to provide a more in-depth understanding of the role of waste banks in overcoming these challenges. With the existence of waste banks, it is hoped that the community will be more aware of the importance of sorting waste and more active in recycling activities, which in turn supports the achievement of sustainable development goals, especially in environmental and economic aspects (Khair, 2019; Saleh et al., 2020). Therefore, this study aims to explore the implementation of the performance of waste banks from economic, social, and environmental aspects, as well as the sustainability strategy of waste banks in Makassar City.

2. METHODS

The case study location is in Makassar City, South Sulawesi, more precisely at the Makassar City Central Waste Bank. The population of Makassar City is 1,477,861 inhabitants (Badan Pusat Statistik Kota Makassar, 2025). Makassar City Central Waste Bank was chosen as the case study location due to its strategic role and prominence in the city's waste management system. As the central hub for waste banking in Makassar, it serves as a key model for other waste banks in the town. It provides a comprehensive data source on the waste bank's operations, management, and community involvement. The central waste bank serves multiple sub-districts within the city and handles a significant volume of waste. This makes it an ideal site for examining how waste banks function at scale and contribute to the city's overall waste management efforts.

The data used in this study includes both secondary and primary data. Secondary data was collected through literature studies and documents from the Central Waste Bank, which provided information on the number of waste bank units in each sub-district, waste sales rates, and waste generation data. Primary data was gathered through observations and interviews with waste bank managers. One limitation of this research is that interviews were not conducted with the users of the waste banks. The data collected was then analysed using qualitative descriptive analysis.

3. RESULT AND DISCUSSION

Waste banks in Makassar City were formed due to the Makassar Green and Clean (MGC) movement and ministerial regulation no. 13 of 2012 to implement the 3Rs through waste banks (Hermansyah, 2021). The Makassar City Waste Bank was introduced and started operating in 2015. Initially, 188 unit waste banks were established and spread across 14 sub-districts. Waste banks accept plastic, paper, metal, and glass types of waste.

People who want to sort and sell their waste must register as members. Generally, the types of waste banks in Makassar City consist of unit, school, sectoral, and waste banks of Regional Work Units/government institutions. These waste banks will later bring the waste collected to the central level, namely the Makassar City Central Waste Bank, for resale. The difference between the unit waste bank and the sectoral waste bank

is that the unit waste bank is a waste bank that serves the urban village and neighbourhood level. This waste bank also accepts individual members (Chanigo, 2023; Yustiani & Abror, 2019). While the sectoral waste bank is a sub-district level service, it can also assist the unit waste bank in sales (Ashariani, 2021), but this waste bank also accepts individual customers. Recorded in 2024, the number of waste banks in Makassar City amounted to 1,212 units, but not all are active. The number of active waste banks each year can be seen in the following table.

Table 1. Number of active waste banks in Makassar City

Year	Number of active waste banks (unit)				Total bank active waste
	Unit Waste Bank	School Waste Bank	Sectoral Waste Bank	Government Institutions	
2015	187	0	1	0	188
2016	243	5	3	2	253
2017	136	155	5	20	316
2018	49	16	0	3	68
2019	27	22	0	10	23
2020	64	27	0	0	91
2021	64	27	0	0	91
2022	64	27	0	0	91
2023	247	39	0	30	316
2024	266	43	0	39	348

(Source: UPT. Bank Sampah Pusat Kota Makassar, 2024)

The data above shows the activeness of waste banks in Makassar City in the last 10 years. The activeness of waste banks in Makassar City experienced a fluctuating trend, 2017 and 2024 showed the highest numbers with 316 and 348 units, respectively, while from 2020 to 2022, the data was stagnant, and there was no increase in the number of active waste banks as a result of the Covid-19 pandemic. Research by (Latanna, 2019) also shows that the impact of the pandemic has reduced activity at Makassar City's waste bank. Besides that, many waste bank units have moved to app-based waste trades, such as MallSampah, and stand independently because it is more efficient during the pandemic and has many advantages. However, in recent years, there has been a significant increase in the activeness of waste banks, especially in the types of unit waste banks and government institutions waste banks.

In buying and selling waste at the central waste bank, each waste bank manager brings their waste to the central waste bank for resale. The waste is then exchanged for money, and the price is based on the weight of the waste. For example, unit waste banks usually collect waste in one month. After collecting a large amount of waste, the unit waste bank manager will contact the central waste bank to pick it up and sell it back to the central waste bank. Trucks or three-wheeled motorised carts will transport the waste to the central waste bank and place it in the dropping area to be sorted and cleaned again. A clearer scheme of the waste buying and selling process at the Central Waste Bank can be seen in the following figure.



Figure 1. The process of buying and selling waste at the Makassar City Center Waste Bank

All waste collected by the Central Waste Bank will be resold to vendors. The central waste bank in Makassar City works with 11 vendors to resell and recycle waste. The vendors are UD. Dua Jaya, UD. Sumber Box, UD. Celebes Agung Niaga, MFC. Mitra Fajar Cemerlang, Hamparan Plastik Gowa, Botol Vendor, Olymplast, Anugrah Vendor, Hadado Go Green, MEP, and Myra Rahma. These vendors will take the waste to Surabaya, Jakarta, and China for recycling. Therefore, the central waste bank in Makassar City only plays a major role in the waste sorting component; it is left to the vendors who have collaborated for other processing. This is a limitation, as the waste bank does not engage in direct recycling processes at the unit or central levels. This lack of direct involvement in recycling means that the waste bank's contribution to the recycling chain is limited to sorting, and it relies on external vendors for the next crucial step in waste management.

The purchase price of inorganic waste by the Makassar City Central Waste Bank is differentiated from the type of waste based on its material. Inorganic waste is categorised into several main groups: plastic, metal, paper, glass bottles, and waste cooking oil. Each of these categories has a varying price depending on the characteristics and reuse value of the material. Plastic waste is classified based on the type and condition of the packaging, such as clear glass, bottles, plastics, and jars, and it has a purchase price range of Rp. 1,000 - Rp. 6,000 per kg, with the highest price for clean, unlabeled clear glass at Rp. 6,000 per kg, and the lowest price for dirty plastic is Rp. 1,000 per kg. Metal materials include iron, aluminium, copper, brass, and bronze. Metal prices are much higher than plastic, with copper from cables having the highest value of Rp. 80,000 per kg, and zinc-iron has the lowest price of Rp. 1,500 per kg. The paper waste category includes white paper, mixed paper, cardboard, newspapers, and cones, with a price range of Rp. 400 – Rp. 1,600 per kg. Glass waste is classified based on the type of beverage previously packaged (glass bottles). The price per bottle ranges from Rp. 250 - Rp1,000 per bottle. Waste cooking oil has a high price, which is Rp. 3,600 per kg. The unit-scale waste bank manager can earn around Rp 1,000,000 - Rp. 2,000,000 per month from the waste sold to the central waste bank. The results of waste purchases by the central waste bank over the past 9 years can be seen in the following figure.

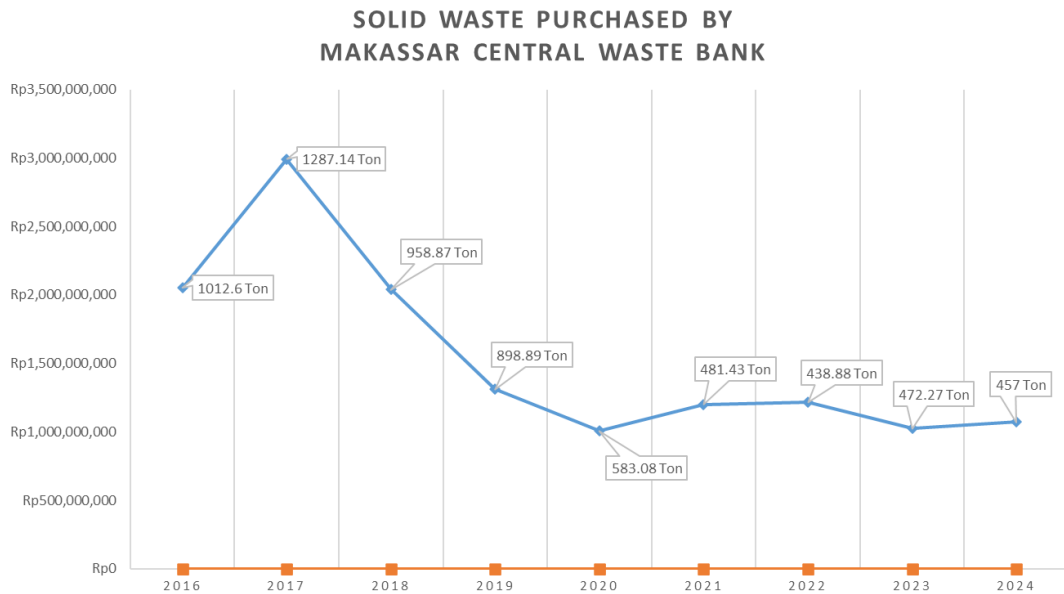


Figure 2. Waste purchased by Makassar City Central Waste Bank in 2016-2024

The data above shows the trend of waste purchase by Makassar Central Waste Bank from 2016 to 2024, which shows a fluctuating pattern with three phases: a significant increase in 2016-2017, a sharp decline in 2018-2020, and stagnation in 2021-2024. At the beginning of the period, the amount of waste purchased experienced a high increase, with the amount of waste collected in 2016 amounting to 1,012.6 tons and in 2018 reaching a peak of 1,287 tons; this was due to increased community participation with the new waste sorting policy supported by an incentive system. However, from 2018 to 2020, there was a decrease in waste purchases due to reduced unit waste bank activities. In addition, research by (Kubota et al., 2020) found that waste collection decreased in 2018 because this was the year of the new mayoral election. This led to differences in political party preferences, with waste bank leaders expressing support for certain candidates while waste bank unit collectors had other preferred candidates. These differences affected the motivation to participate in the waste bank program.

The years 2020-2024 showed a pattern that tended to stagnate. Although there were slight fluctuations, in general, the amount of waste purchased did not experience a significant increase. This is supported by Hermansyah's research, 2021, which concluded that community participation in processing waste in 2021 was around 27.33%, which is classified as low (Hermansyah, 2021). This condition shows that challenges have not been resolved in increasing the waste collected.

3.1 Evaluation of Makassar City Waste Bank Management

The evaluation of waste bank management in Makassar City uses the standard components of waste bank management from the Ministry of Environment Regulation No. 13 of 2012, which consists of assessing the components of members, waste bank organisers, waste collectors/buyers/recycling industries, management in waste banks, and the role of waste bank managers (Kementerian Lingkungan Hidup, 2012). The evaluation results are displayed in table form and explained as follows.

Table 2. Evaluation of Makassar City Waste Bank management

Component	Sub-component	Existing condition
Members	Waste bank counseling is conducted at least 1 (one) time in 3 (three) months	X
	Each member is given 3 three sorting waste packages	X

Component	Sub-component	Existing condition
	Members get an account book and garbage savings account number	✓
	Have done waste sorting	✓
	Have made efforts to reduce waste	✓
Waste bank organiser	Use Personal Protective Equipment (PPE) while serving members	X
	Wash hands with soap before and after serving waste savers	X
	Have participated in waste bank training	✓
	Number of daily managers at least five employees	X
	Managers get a salary/intensive every month	✓
Waste collector/buyer/recycling industry	No burning of waste	✓
	Has a cooperation/MoU with a waste bank as a partner in waste management	✓
	Able to maintain environmental cleanliness, such as the absence of mosquito larvae in can/bottle bins	✓
	Have a business license	✓
Waste management in a waste bank	Waste can be picked up by collectors at least once a month	✓
	Waste bank-assisted craftsmen recycle waste worthy of creation	X
	Compostable waste suitable for neighbourhood and/or communal scale management	X
	The number of members increases by an average of 5-10 members every month	X
The role of waste bank managers	As a facilitator in the development and implementation of waste banks	✓
	Provide waste collector/buyer data for waste banks	✓
	Provide recycling industry data	✓
	Reward waste banks	✓

The evaluation results show that several sub-components in the standard are still not implemented. One is the members component, which does not conduct counselling for members regularly, at least once every 3 months. There is no provision for three waste packages for each member, where members pack their waste using plastic bags or rice sacks. The waste bank organiser component, which is based on direct observation, does not wash their hands before and after serving members and does not use PPE. In addition, the average manager is only 2-3 people at the unit-level waste bank.

In the waste management component of the waste bank, the unit, and central-level waste banks, there are no waste recycling activities by craftsmen. Waste management activities only reached the sorting stage; previously, the central waste bank provided composting facilities in each waste bank unit, but unit-level managers did not use this facility due to a lack of knowledge of how to process organic waste into compost properly. The number of additional members also does not increase by 5-10 every month; the increase fluctuates and is erratic.

Based on the results of the above evaluation and observations, as well as interviews in the field, several issues of waste bank management were formulated it is 1) lack of community participation, 2) the non-optimal role of the manager, and 3) inadequate facilities in waste bank management.

The first issue is the lack of community participation due to the lack of knowledge about waste management, awareness, and motivation. Generally, the main reason why people become waste bank members is because they only want to get economic benefits. Most people interested in becoming waste bank members come from the middle to lower economic levels, while the upper middle economic level is still relatively low.

Hence, the importance of socialisation from the waste bank. In addition, since members must bring their waste to the waste bank to be sold, this may not be easy for some people because they have to take their time. Currently, many online waste trader applications have a similar concept to waste banks in Makassar City, one of which is MallSampah. However, from the waste bank itself, both at the central and unit levels, there is no online service to pick up or receive waste. Based on interviews with the waste bank units, some customers are no longer active because they prefer to use online waste trader applications where the buying and selling process is easier and more efficient.

The second issue is that the manager's role is not optimal because the average number of workers in the waste bank unit is only 2-3 people. According to the written standards, waste banks should employ five people. In addition, the obstacle that prevents the waste bank from running well is the lack of supervision and socialisation of the program from the central waste bank. For example, the central waste bank has facilitated unit waste banks with composters to process organic waste on a neighbourhood scale. However, the unit waste bank does not use this facility because of the lack of knowledge on how to process organic waste into compost, such as in the Ujung Tanah sub-district. Several studies (Haerul et al., 2016; Latanna, 2019) show that the waste bank program is considered non-optimal due to a lack of socialization in the community, especially regarding the concept of reuse, reduce, and recycle (3R). As a result, the community does not fully understand the applicable regulations and is not yet strongly committed to changing attitudes towards environmental cleanliness. The lack of adequate education also leads to low active community participation in the waste bank program, which results in a lack of positive impact on sustainable waste management. Based on interviews with the central waste bank, socialisation is not carried out regularly because there is no budget for socialisation.



Figure 3. Composter at the unit waste bank

The third issue is the inadequate waste bank management facilities, especially in waste storage containers. Currently, there are still many waste bank units that do not have adequate storage facilities, so all the waste that has been collected is mixed in one place. As a result, the sorting process must be repeated before the waste is distributed to the central waste bank, which can slow down waste management efficiency. In addition, due to the absence of storage facilities, some waste bank units also put the collected waste on vacant land, which reduces the aesthetics of the environment and has the potential to cause environmental impacts.



Figure 4. Waste collection in the waste bank unit

Limited waste storage facilities occur not only at the unit level but also at the central level. Although the central waste bank has provided a dropping area designed to separate waste by type, the area's capacity is still insufficient to accommodate the entire volume of incoming waste. Managers are forced to place waste in empty areas around the facility.



Figure 5. Dropping area at the central waste bank

In addition, based on the standard, each member is supposed to receive three types of waste packaging to sort waste from the source. However, members have not received such packaging and are forced to provide their own packaging for the waste they intend to sell. Generally, members use plastic bags and rice sacks, which is against the basic principle of waste banks in reducing plastic waste. In addition, waste bank units in the islands of Makassar City face an additional challenge in transporting their waste to the central waste bank because they have to provide their own boats. Without adequate transportation facilities, such as specialised motorboats, the operations of unit waste banks in small islands become even more difficult. This lack of standardised facilities has resulted in the waste sorting process not running optimally.

3.2 Strategies for a Sustainable Waste Bank

Developing an effective waste bank management strategy is important for sustainable waste management. These strategies arise from issues such as community participation in waste management, the unoptimised role of waste bank managers, and inadequate facilities in supporting waste bank operations. Therefore, this section will discuss some strategies that can be implemented to ensure that the Makassar City Central Waste Bank can operate effectively and sustainably.

The first strategy is that public participation must be strongly encouraged. Public participation can be increased by counselling or socialising about the importance of managing waste, processing, types of waste, and information about waste banks. This socialisation does not have to be done directly. However, it can be done through posts and social media, such as the one done by Bersinar Waste Bank, Bandung City. The operations of Bersinar Waste Bank were effective (Kusumawati et al., 2019). Bersinar Waste Bank has a website that contains information related to waste banks. In addition to the website, Bersinar Waste Bank has

an Instagram social media page containing forms for customer registration, waste pickup, and waste sorting guidelines. Previously, the Makassar City Central Waste Bank already had an Instagram social media account. However, the account was not actively used, so it is hoped that the account will be activated. It will post much information to the public about how to become a member of the waste bank and education related to waste management. In addition, counselling or socialisation can also be done by holding online seminars. Bersinar Waste Bank often holds online seminars on waste management and introductions related to waste banks. In addition, waste banks can also work with institutions to provide information about waste management and empower young people to carry out environmental care movements through waste banks.

Education is pivotal in fostering creativity and innovation within the community, especially in transforming waste into valuable products with economic benefits. This approach can significantly optimise waste management practices and create a sustainable city (Fatmawati et al., 2022). Aside from the success of Bersinar Waste Bank, the tangible benefits of waste management education are evident in Kamikatsu City, Japan. Since 2002, Kamikatsu has implemented a zero-waste management system, where waste is sorted centrally and 100% composted at the household level (Jarman-Walsh, 2019). The city has successfully applied the 5R principles: refuse, reduce, reuse, recycle, and recover, with everyone, from young to old, having been educated on the importance of living waste-free. As a result, residents understand the severe environmental impact of pollution and have embraced the zero-waste lifestyle in their daily routines (Sidjabat & Ilmi, 2020).

The second strategy is the reaffirmation of waste sorting regulations. Waste sorting is a critical initial step in waste management, as outlined in the Makassar City Regional Regulation No. 4/2011 on Waste Management. This regulation mandates waste sorting as an obligation for all community members. To strengthen compliance and ensure effective waste management, a policy requires the community to sort waste through the waste bank system. Reaffirming this regulation will encourage consistent waste sorting among individuals and institutions, making waste management more organized and effective.

The third strategy is to improve the performance and role of waste bank managers. One of the important factors in the success of waste banks is their professional and efficient management. Therefore, the standard operating procedures for waste bank management must be updated and reaffirmed to ensure optimal implementation. Building close partnerships between waste banks and other stakeholders, as well as providing ongoing training and coaching to waste bank management staff, is essential to improve the ability of managers to manage waste properly. In addition, it is important to regularly monitor and evaluate all programs run by the waste bank. All activities must be recorded properly as a basis for assessing the success of the waste bank. As a form of appreciation for successful waste banks, appropriate awards should be given to encourage motivation to improve their performance. Waste banks also need to support the development of waste recycling craftsmen to increase the economic value of the processed waste. In addition, waste banks should introduce digital platforms to facilitate online transactions and collection services so that people can still participate in waste management programs even in limited conditions.

The fourth strategy is to improve waste bank facilities and infrastructure. Providing adequate facilities and infrastructure is important to support effective waste bank operations. Waste banks must provide sorting containers that follow established waste management standards. In addition, operational equipment such as waste containers, shredders, composters, and other facilities must be provided completely and adequately in each waste bank unit. In this context, Makassar City Regional Regulation No. 4/2011 mandates that providing adequate facilities and infrastructure will support the achievement of waste reduction targets. Therefore, waste banks must collect data on the completeness and quality of their waste facilities and conduct regular maintenance to ensure that waste bank operations go well.

4. CONCLUSIONS

The implementation of the Central Waste Bank in Makassar City has shown quite good economic results because it can increase the income of the community, especially the lower-middle income, and succeed in

reducing waste. Nevertheless, some issues still need to be addressed, including the lack of community participation, services and the role of waste bank managers that are not yet optimal, and facilities that support the operations of waste banks that are not yet adequate. Based on the study results, it can be concluded that waste banks in Makassar City have fulfilled two of the three pillars of sustainability, namely the economic and environmental aspects, but have not fully fulfilled the social aspects. One of the main reasons is the lack of active participation from the community in the program. Community participation is crucial in ensuring that waste banks function optimally, but low awareness and understanding of the importance of waste management can hinder the program's success. Therefore, waste banks in Makassar City have not yet reached the expected level of sustainability.

Several strategies need to be implemented to achieve better sustainability and support the achievement of targets 3 and 8 of the SDGs related to circular economy. First, community participation should be encouraged more intensively through direct socialisation and using social media and webinars to educate the importance of waste management. Second, waste sorting regulations must be an affirmation to ensure community compliance with more structured waste management. Third, the role of waste bank managers needs to be strengthened by training and increasing operational capacity. Fourth, adequate facilities and infrastructure should be prioritised to support operational activities and increase waste banks' effectiveness in Makassar City.

Although this article provides valuable insights, it acknowledges its limitations. This study does not fully capture the experiences and perspectives of waste bank users regarding the system's effectiveness and its impact on their waste sorting habits and overall well-being. To address this limitation in future research, it would be beneficial to include interviews or surveys with waste bank users to gather direct feedback on their experiences.

5. ACKNOWLEDGMENTS

The author would like to thank the Makassar City Central Waste Bank Manager and the Makassar City Waste Bank Unit for their valuable contribution in providing in-depth data and information for this research

REFERENCES

- Aminah, N. Z. N., & Muliawati, A. (2021, August 27). *Pengelolaan Sampah dalam Konteks Pembangunan Berkelanjutan (Waste Management in the Context of Waste Management)*. <https://hmgp.geo.ugm.ac.id/2021/08/27/pengelolaan-sampah-dalam-konteks-pembangunan-berkelanjutan-waste-management-in-the-context-of-waste-management/>
- Ashariani, R. (2021). Strategi Pengelolaan Bank Sampah Sektor Kecamatan Tallo Kota Makassar. *Repository Universitas Negeri Makassar*. http://eprints.unm.ac.id/23467/1/JURNAL_RESKI_ASHARIANI.pdf
- Badan Pusat Statistik Kota Makassar. (2025). *Kota Makassar Dalam Angka Tahun 2025*.
- Chanigo, R. Y. (2023). Faktor yang Mempengaruhi Kinerja Bank Sampah di Indonesia. *Teknik Lingkungan*, 9(1), 107–115.
- Dinas Lingkungan Hidup Kota Makassar. (2024). *Laporan Akhir Kajian Persampahan Limbah Domestik Kota Makassar tahun 2024*.
- Fatmawati, F., Ilham, I., Saleh, S., & Razak, A. R. (2024). Waste Management System: A Case Study of Waste Bank Management Toward a Circular Economy in Maros Regency. *Jurnal Borneo Administrator*, 20(1), 1–14. <https://doi.org/10.24258/jba.v20i1.1206>
- Fatmawati, F., Mustari, N., Haerana, H., Niswaty, R., & Abdillah, A. (2022). Waste Bank Policy Implementation through Collaborative Approach: Comparative Study—Makassar and Bantaeng, Indonesia. *Sustainability (Switzerland)*, 14(13). <https://doi.org/10.3390/su14137974>
- Haerul, Akib, H., & Hamdan. (2016). Implementasi Kebijakan Program Makassar Tidak Rantasa (MTR) di Kota Makassar. *Jurnal Administrasi Publik*, 6(2), 21–34.
- Hermansyah, H. (2021). *Evaluasi Kinerja Bank Sampah Dalam Pengelolaan Sampah di Kota Makassar*. Universitas Hasanuddin.

- Jarman-Walsh, J. (2019). Foundations of Zero-Waste Lead to Sustainable Tourism Success: The Case of Kamikatsu. *安田女子大学紀要*, 249–260.
- Kementerian Lingkungan Hidup. (2012). *Peraturan Menteri Lingkungan Hidup Nomor 13 Tahun 2012 tentang Pedoman Pelaksanaan Reduce, Reuse, dan Recycle Melalui Bank Sampah*. <http://jdih.menlhk.co.id/>
- Kementerian Lingkungan Hidup dan Kehutanan. (2021, August 13). *Menteri LHK: Pengelolaan Lingkungan Bisa Tersesat Bila Hanya Modis, Figuratif dan Ilustrasi!* <http://ppid.menlhk.go.id/berita/siaran-pers/6116/menteri-lhk-pengelolaan-lingkungan-bisa-tersepat-bila-hanya-modis-figuratif-dan-ilustrasi>
- Khair, H. (2019). *Study on Waste Bank Activities in Indonesia Towards Sustainable Municipal Solid Waste Management* [The University of Kitakyushu]. https://kitakyu.repo.nii.ac.jp/index.php?action=pages_view_main&active_action=repository_action_common_download&item_id=714&item_no=1&attribute_id=20&file_no=1&page_id=13&block_id=294
- Kubota, R., Horita, M., & Tasaki, T. (2020). Integration of community-based waste bank programs with the municipal solid-waste-management policy in Makassar, Indonesia. *Journal of Material Cycles and Waste Management*, 22(3), 928–937. <https://doi.org/10.1007/s10163-020-00969-9>
- Kusumawati, R., Gunawan, S., & Julimawati. (2019). Efektivitas Bank Sampah Bersinar Dalam Kepedulian Pengelolaan Sampah dan Peningkatan Ekonomi Masyarakat (Studi Kasus: Bank Sampah di Kelurahan Baleendah, Kecamatan Baleendah). *Gearea*, 2(2), 1–11.
- Latanna, M. D. (2019). *The Evaluation of Community-Based Solid Waste Management (Waste Bank) Program in Makassar, South Sulawesi, Indonesia*. University of Twente.
- Masruroh, Sri Nuraeni, N., Rio Pambudi, M., Iqbal Liayong Pratama, M., & Hendra. (2022). The Socio-Economic Impact of Waste Bank Program in Banten Province. *Jurnal Geografi Gea*, 22(2), 106–116. <https://ejournal.upi.edu/index.php/gea/article/view/48853/20474>
- Nur, H. (2021, August 18). *Circular Economy, Upaya Mengelola Sampah Plastik dalam Bisnis Berkelanjutan Universitas Indonesia*. <https://www.ui.ac.id/circular-economy-upaya-mengelola-sampah-plastik-dalam-bisnis-berkelanjutan/>
- Rumata, N. A., Julianti, D. R., & Janna, N. M. (2025). Strategi Pengelolaan Sampah di Kawasan Permukiman Lantebung Kota Makassar. *Journal of Green Complex Engineering*, 2(2), 97–103.
- Rusni, N. K. (2024). Permasalahan Sampah Kota Makassar Studi Kasus TPA Tamangapa. *Waste Handling and Environmental Monitoring*, 1(1), 16–27. <https://doi.org/10.61511/whem.v1i1.2024.511>
- Saleh, H., Surya, B., & Hamsina, H. (2020). Implementation of sustainable development goals to makassar zero waste and energy source. *International Journal of Energy Economics and Policy*, 10(4), 530–538. <https://doi.org/10.32479/ijee.9453>
- Satori, M., Amaranti, R., & Srirejeki, Y. (2020). Sustainability of waste bank and contribution of waste management. *IOP Conference Series: Materials Science and Engineering*, 830(3). <https://doi.org/10.1088/1757-899X/830/3/032077>
- Schroeder, P., Anggraeni, K., & Weber, U. (2019). The Relevance of Circular Economy Practices to the Sustainable Development Goals. *Journal of Industrial Ecology*, 23(1), 77–95. <https://doi.org/10.1111/jiec.12732>
- Setyarini, S. V., Subowo, A., & Afrizal, T. (2020). Program Bank Sampah Dalam Upaya Pembangunan Berkelanjutan di Kabupaten Semarang (Studi di Bank Sampah Soka Resik, Dusun Soka, Desa Lerep, Kecamatan Ungaran Barat, Kabupaten Semarang). *Journal of Public Policy and Management Review*, 10(1), 252–261. <https://doi.org/10.14710/JPPMR.V10I1.29795>
- Sidjabat, F. M., & Ilmi, A. (2020). Kamikatsu Japan's Ecovillage Conceptual Framework for Environmental Management (Case Study: Lake Ciburuy, West Java, Indonesia). *Journal of Physics: Conference Series*, 1625(1). <https://doi.org/10.1088/1742-6596/1625/1/012063>
- Susan, L., Azwar, & Al-Adaliah, R. (2023). Edukasi Pengolahan Sampah Rumah Tangga Menuju Kota Makassar Sehat Dan Hijau. *Jurnal Keuangan Umum Dan Akuntansi Terapan (Jurnal Kuat)*, 5(2), 121–126.
- UPT. Bank Sampah Pusat Kota Makassar. (2024). *Data Bank Sampah Pusat 2024*.
- Wulandari, D., Utomo, S. H., & Narmaditya, B. S. (2017). Waste bank: Waste management model in improving local economy. *International Journal of Energy Economics and Policy*, 7(3), 36–41.
- Yustiani, Y. M., & Abror, D. F. (2019). Operasional Bank Sampah Unit Dalam Pengelolaan Sampah Perkotaan. *JURNALIS: Jurnal Lingkungan Dan Sipil*, 2(2), 82–89.